

NO. 67-111

INSTRUMENTATION
LABORATORY

Reproduced by the
CLEARINGHOUSE
for Federal Scientific & Technical
Information Springfield Va. 22151

E-2319

CALCULATION OF THE GRAVITY FALL MOTION
OF A MOORING SYSTEM

by

Michel R. Froidevaux

Roger A. Scholten

August 1968

INSTRUMENTATION LABORATORY
MASSACHUSETTS INSTITUTE OF TECHNOLOGY
CAMBRIDGE, MASSACHUSETTS 02139

Approved:

Roger B. Woodbury
ROGER B. WOODBURY, DEPUTY DIRECTOR
INSTRUMENTATION LABORATORY

Date:

12/9/68

ACKNOWLEDGMENT

This report was prepared under DSR Project 53-30200, sponsored by the Office of Naval Research, Department of the Navy, under Contract NONR 3963 (31) with the Instrumentation Laboratory, Massachusetts Institute of Technology, Cambridge, Massachusetts.

The authors wish to express their sincere appreciation to Mr. John Dahlen, director of the Oceanography program at the MIT Instrumentation Laboratory for his numerous helpful technical comments throughout the realization of the present work.

The authors also express their gratitude to Mr. Walker Kupfer, also of the MIT Instrumentation Laboratory, for his careful proof-reading and constructive criticism.

The typing of the manuscript was ably undertaken by Miss Ethel Fistes. Her skill and perseverance are greatly appreciated.

The publication of this report does not constitute approval by the Office of Naval Research of the findings or the conclusions contained therein. It is published only for the exchange and stimulation of ideas.

CALCULATION OF THE GRAVITY FALL MOTION OF A MOORING SYSTEM

ABSTRACT

→ Fast digital computational methods enable solution of the system of non-linear partial differential equations describing the free fall motion of a mooring system. The problem is initially approached by a simplified model in which the distributed mass of the cable has been lumped in a series of discrete masses attached to a weightless line. Also, the more general mooring configuration analyzed in this report includes floats (for which the buoyancy is considered uniformly distributed and then re-distributed into lumped discrete negative weights), cables which can be either inextensible (steel) or elastic (synthetic line), and an anchor which is assumed of spherical shape. The simulation results are presented for several different specific cases, but in order to minimize the computational cost, most of the textual material is derived from the comprehensive analysis of a single relatively short mooring system. These results are extrapolated to apply to the 6500 foot Oceanic Telescope, which constituted the original purpose of this work (the problem was to investigate the feasibility of the free-fall of such a mooring).

The major contributions of the authors are:

- 1) The flexible character of the three-dimensional program which is designed to handle many possible configurations of moorings as well as further effects of cross-current perturbations or Karman-Vortex-induced lateral motions of the cable.
- 2) The inclusion in the program, for the solid cable case, of the inextensibility condition directly within the tension equation.
- 3) The complete treatment of the elastic case which permits the calculation of the transient motion occurring after the anchor has hit the bottom of the sea.
- 4) The determination of a stable and efficient numerical procedure using a tension-correcting feed-back from boundary conditions at the anchor which minimizes the amount of iteration.

The conclusion of immediate practical interest is that the free drop of the Oceanic Telescope would involve excessive risk due to overstress at one portion of the cable and the possibility of an undesirable transient at impact.

It may also be concluded from this report that elasticity properties of the cable do not appreciably affect the time of fall or the general shape of the falling cable. It is necessary to include elasticity in studying the tension histories, especially at the time immediately following anchor impact when the tension may rise to critical values.

by
Michel R. Froidevaux
and
Roger A. Scholten

CALCULATION OF THE GRAVITY FALL MOTION
OF A MOORING SYSTEM

By Michel R. Froidevaux and Roger A. Scholten

TABLE OF CONTENTS

- I. Introduction
- II. Derivation of the general equations of motion
 - A. Non-elastic cable equations
 - B. Modified equations for the elastic cable
- III. Description of computational procedure
 - A. Programming the non-elastic model
 - B. Modifications of standard program to obtain transient motion after anchor impact
 - C. Programming the elastic fall
- IV. Simulation results
 - A. Non-elastic cable fall
 - B. Elastic cable fall
- V. Conclusions and recommendations for further studies
- Appendix A: Programming notations and symbols
- Appendix B: Consideration on numerical stability
- References

BLANK PAGE

I. Introduction

In the recent past, attention has been given to the study of flexible cables and their general equilibrium configuration and tensions in various flowfields. Much of the early literature on the subject stems from the work of H. Glauert¹ who published his papers on the stability of an airborne, nonlifting towed vehicle in rectilinear motion in 1930. His prior assumptions were steady-state aerodynamics and constant tow-vehicle velocity which eliminated time from all the equations and thus enabled a closed-form hand calculation of the cable shape. More recently, Walton and Polachek² implemented a numerical solution for the calculation of transient motion of submerged cables subjected to fixed boundary conditions (positions of end points known at all times). This was carried out as a generalization of the classical vibrating string problem. It is a major reference for better understanding of the present report.

With a computer solution in mind, in this paper the authors derive the basic equations governing the hydrodynamic fall of the mooring and present them in a simple form. Equally important, they present a flow-chart of the computational process to clarify the digital solution in its simplest form (non-elastic cable). Forces that are assumed acting on the cable are: (a) Reaction at the fixed attachment point at one extremity of the cable, (b) damping or drag as the cable falls through the fluid, and (c) inertial reaction of the surrounding fluid and weight or buoyancy of the mooring system which includes a massive anchor at the free extremity of the cable. There are no restrictions on the size of displacements and no approximations are made in any of the governing equations of the program. This enables a great flexibility of computation and presents capability for practical application. The report is presented so that the most straightforward non-elastic case appears first. The motions here can be calculated using relatively long time increments, provided that all significant components of the driving forces lie in the frequency range well below the lowest natural frequency of the model system. (Practically, all the cable modes are more or less excited by non-perfectly stable initial conditions.) In the more general case of the elastic cable, the computational time increments have to be very small to allow tracking the longitudinal vibration waves of the mooring line. This subsequently increases the overall computational time and economically prohibits the calculation of the full drop history. Only the first second of fall and the first second following the impact of the anchor were investigated. Nevertheless, these histories present a comprehensive amount of information for the derivation of conclusions.

A MAC* language computer program was written to study the application of the theoretical equations to several cases of interest. It permits an elegant and concise digital solution to the hydrodynamic problem because all the equations are easily formulated in terms of vectors. All the curves and charts have been drawn from MAC runs.

The available program, although designed to determine the gravity fall motion of a mooring system, provides an applicable solution to a wide class of other engineering problems involving the motion of cables.

This study was initially prompted by a desire to more rationally estimate the risk associated with free-fall implantment of the Oceanic Telescope Outer Moorings. See figure 1 for a schematic drawing of the Oceanic Telescope. It was concluded that a free-fall implantment might involve an overstress shortly after the drop and an extreme transient at impact with the ocean floor. Until further study can be undertaken, the anchor-first technique will be employed.

*MAC is an algebraic computer language developed at the MIT Instrumentation Laboratory for engineering applications. It has a basic 3-line format but otherwise is similar to the more generally used Fortran.

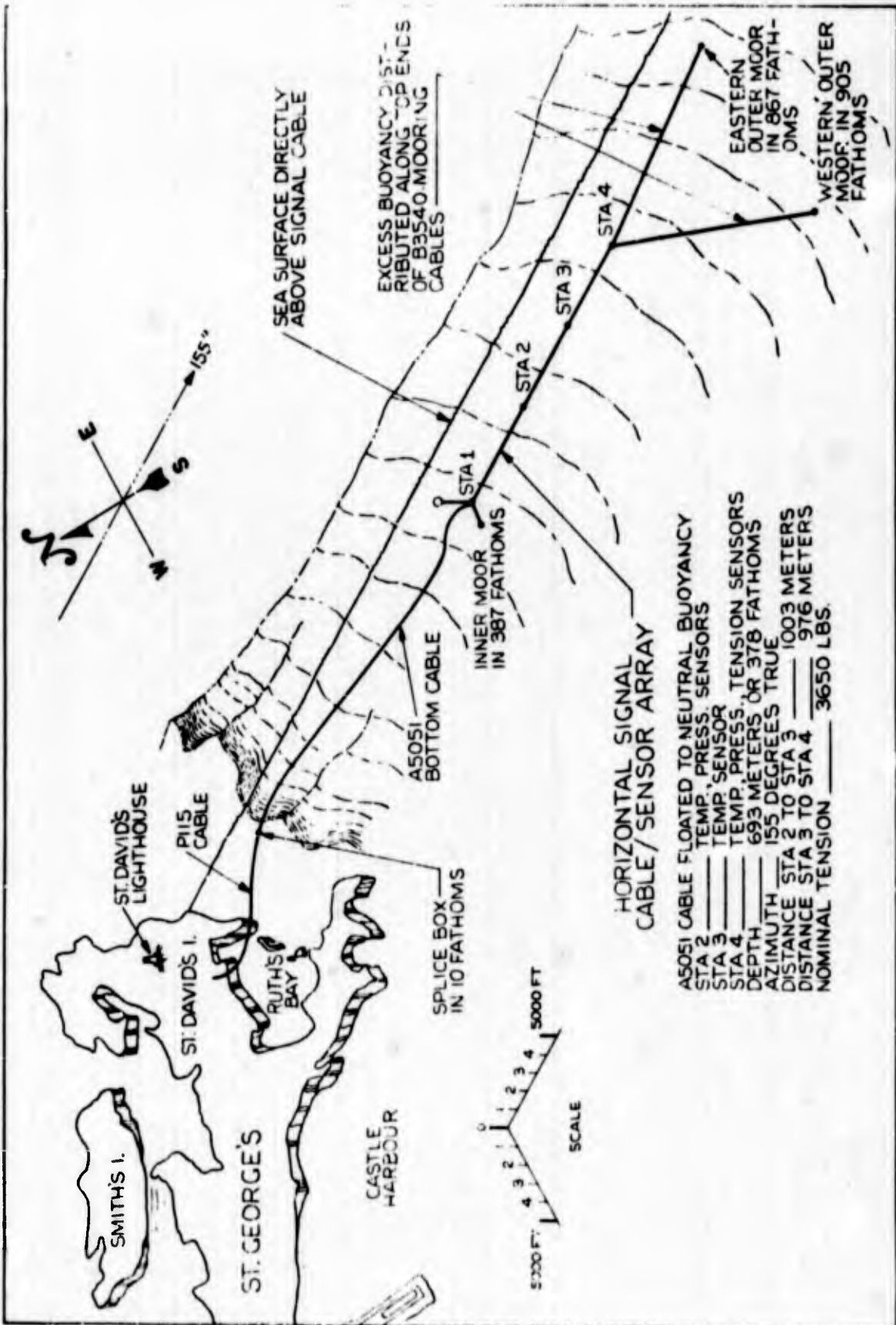


Fig. 1

II. Derivation of the Equations of Motion

A. Non-Elastic Cable Equations

The Runge-Kutta method of numerical integration, based on finite-difference approximations, is available within the automatic library of the computer. It uses finite-differences in the time domain, and thus leads to the possibility of using finite lengths in the space dimensions. It is therefore natural to introduce space discreteness into the original formulation of the problem and thus to present the equations of motion of a simplified model in which the distributed mass of the cable is replaced by a series of discrete masses M_k attached to a weightless, inextensible line. This leads to a system of ordinary differential equations.

Figure 2 shows a typical configuration of the system, before and after the anchor drop. It is assumed that one extremity of the cable remains fixed at the surface at all times.

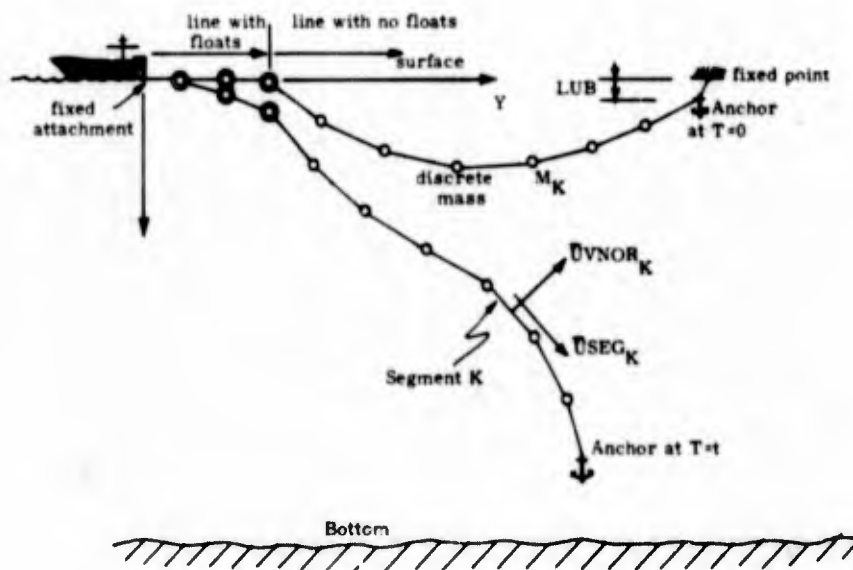


Fig. 2 Mooring line simplified model.

All the equations were formulated in vector form. It is therefore necessary to define two directions related to the cable by means of two unit vectors (at present, motion can be assumed to take place in the vertical plane).

\bar{U}_{SEG_k} : unit vector at the center of segment k in the vertical plane, the direction of which is parallel to segment k , positively toward the anchor.

\bar{U}_{VNOR_k} : unit vector at the center of segment k in the vertical plane, the direction of which is normal to segment k , positively toward the surface of the ocean.

Figure 3 shows the segment and node numbering system adopted for computational purpose as well as the external forces acting on node k , with the proper sign convention for the tensions. The junctions between the segments are numbered according to the subscript index k , which runs from 0 at the boat to S at the anchor.

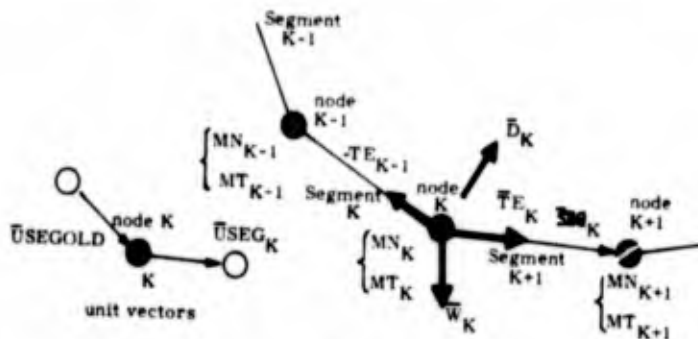


Fig. 3

Also, it should be noted that the positive X direction is chosen to be directed toward the bottom of the ocean and that the positive Y axis lies on the surface of the water as indicated on figure 1.

When considering the inertial properties of the fluid in which the cable is immersed, it is assumed that the kinetic energy imparted to the surrounding medium varies as the square of the component of velocity normal to the line and that it is almost independent of the component of velocity parallel to the line, although the same law with a tangential drag coefficient 50 times smaller than in the normal direction is used as an approximation.

That is, for the cable,

$$DNC = 1/2 RHOSW A_N CDN VN^{2*} \quad \text{and,} \quad (2.1)$$

$$DTC = 1/2 RHOSW A_T CDT VT^2 \quad (2.2)$$

with $CDT = 0.02 CDN$

For the calculation of the equivalent mass of the fluid entrained with each segment (sometimes referred to as the virtual mass), the additional mass in a direction parallel to the cable is considered to be 1/50 the additional mass normal to the cable so that for the augmented mass of one foot of cable, we have:

$$UMCN = UMC (1 + 9/46) \quad (2.3)$$

$$UMCT = UMC (1 + 0.02 \ 9/46) \quad (2.4)$$

* See Appendix for definitions of the parameters which appear in equations. (Programming notation)

The (9/46) coefficient is calculated from the expression for the virtual mass:

$$M_v = \rho k v \quad (3)$$

where v is the volume of the moving body

ρ is the density of the fluid

$k = 0.5$ for a sphere and $= 1$ for a cylinder.

For the cylindrical cable, the ratio of the specific mass of sea water to that of the metal cable is roughly 9/46 and thus, the augmented mass is given by:

$$UMCN = v\rho_c \left[1 + \rho/\rho_c \right]$$

where ρ_c refers to the cable.

Each lumped mass (MN, MT) has been expressed as half the mass of the segment on one side of the node plus half of the mass of the segment on the other side of the node, including the equivalent masses of the fluid entrained.

The vector force acting on node k can then be expressed as the sum of four vectors: the 2 tensions acting along the adjacent segments (internal forces), the weight and the hydrodynamic reaction or drag force (external forces), as shown on figure 3. Newton's law of motion can now be invoked in vector form for the lumped mass k : The acceleration in the normal direction is given by:

$$AN_k = (\bar{T}E_k - \bar{T}E_{k-1} + \bar{D}_k + \bar{W}_k) \cdot \bar{U}VNOR_k / MN_k \quad (2.5)$$

The acceleration along the tangential direction is expressed as:

$$AT_k = (\bar{T}E_k - \bar{T}E_{k-1} + \bar{D}_k + \bar{W}_k) \cdot \bar{U}SEG_k / MT_k \quad (2.6)$$

(where \bar{W}_k can be representative of a weight or a buoyancy force),

If we let \bar{F}_k be the sum $(-\bar{T}E_{k-1} + \bar{D}_k + \bar{W}_k)$, we can write the equation of motion in a more concise form:

$$\bar{A}_k = \left[(\bar{F}_k + \bar{T}E_k) \cdot \bar{U}SEG_k / MT_k \right] \bar{U}SEG_k + \left[(\bar{F}_k + \bar{T}E_k) \cdot \bar{U}VNOR_k / MN_k \right] \bar{U}VNOR_k \quad (2.7)$$

where

$$\bar{F}_k = \bar{T}E_{k-1} + \bar{D}_k + \bar{W}_k \quad (2.8)$$

which is the form used in the computer program.

In the expressions (2.5) and (2.6) the drag forces D_k is also computed by summing the effect on the two half-segments connecting at node k and are rewritten as:

$$D_k = 1/2 (DN_{k-1} + DN_k + DT_{k-1} + DT_k) \quad (2.9)$$

As mentioned previously, it was assumed that all drag forces were proportional to the square of each component of relative velocity with a very small drag coefficient in the direction parallel to the line ($DNC_k = 50 DTC_k$)

$$\bar{D}N_k = - DNC_k \left| VNOR_k \right| VNOR_k \bar{U}VNOR_k \quad (2.10)$$

$$\bar{D}T_k = - DTC_k \left| VT_k \right| VT_k \bar{U}SEG_k \quad (2.11)$$

where the velocity at the midpoint of each segment ($\bar{V}MP$) is taken as a representative value for the computation of the drag force related to the full segment. Thus:

$$VNOR = \bar{V}MP \cdot \bar{U}VNOR \quad (2.12)$$

$$VT = \bar{V}MP \cdot \bar{U}SEG \quad (2.13)$$

The use of the minus sign and the introduction of the absolute value of one of the scalar velocity factors ensures that the drag will always be opposed to the direction of the motion and thus acts as a dissipative force to remove energy from the system.

In equation (2.6), the tensions have yet to be determined.

If one assumes the tension at the fixed point $\bar{T}E_0$ to be known (tension at the boat or TBOAT), then at node 1 all the forces and positions are known from the preceding iteration, (hydrodynamic reactions are computed from the knowledge of positions and velocities) except for the tension to the right of node 1, that is $\bar{T}E_1$, which is calculated next.

Again, if one lets \bar{F}_1 be the sum of forces acting at node 1 except for the tension to the right,

$$\bar{F}_1 = -\bar{T}E_0 + \bar{W}_1 \quad (2.14)$$

One can invoke the inextensibility condition of the cable directly in the equation for the tension by writing that the lumped mass at node 1 cannot accelerate in a direction parallel to $\bar{U}SEG_0$ with respect to point 0, but can only accelerate around the fixed point 0, at a certain given distance lL_1 , from it. In vector notation,

$$\bar{T}E_1 = \left[-\frac{MT_1}{lL_1} \left| \bar{V}_1 - \bar{V}_0 \right|^2 + (MT_1 \frac{d\bar{V}_0}{dT} - \bar{F}_1) \cdot \bar{U}SEGOLD_0 \right] \left[\bar{U}SEG_1 / (\bar{U}SEG_1 \cdot \bar{U}SEGOLD_0) \right] \quad (2.15)$$

Equation (2.15) can be thought of more simply as being derived from the more general relation (at node 1):

$$(\bar{T}E_1 + \bar{F}_1) \cdot \bar{U}SEGOLD_0 = MT_1 \bar{A}_1 \cdot \bar{U}SEGOLD_0 \quad (2.16)$$

which clearly is Newton's law of motion projected along the longitudinal direction. (\bar{A}_1 is the vector acceleration.)

Now, \bar{A}_1 is constrained such that:

$$\bar{A}_1 \cdot \bar{U}SEGOLD_0 = -\frac{\left| \bar{V}_1 - \bar{V}_0 \right|^2}{lL_1} + (d\bar{V}_0/dT) \cdot \bar{U}SEGOLD_0 \quad (2.17)$$

$$\text{Also, } \bar{T}E_1 = TE_1 \bar{U}SEG_1 \quad (2.18)$$

so that from (2.16),

$$TE_1 (\bar{U}SEG_1 \cdot \bar{U}SEGOLD_0) = (MT_1 \bar{A}_1 - \bar{F}_1) \cdot \bar{U}SEGOLD_0 \quad (2.19)$$

Thus it follows that:

$$TE_1 = (MT_1 \bar{A}_1 - \bar{F}_1) \cdot \bar{U}SEGOLD_0 / (\bar{U}SEG_1 \cdot \bar{U}SEGOLD_0) \quad (2.20)$$

The reader may verify that a simple substitution of (2.17) into (2.20) is sufficient to obtain equation (2.15).

The inextensibility constraint, contained entirely in equation (2.15) holds for each segment of the line until the last segment is reached, that is, the anchor.

At that particular point, it is required that no tension exist along the last segment to the right of the anchor. The error tension is computed by the dot product:

$$TE = \bar{TE} \cdot \bar{USEG} \quad (2.21)$$

(A fictitious \bar{USEG} parallel to $\bar{USEGOLD}$ is introduced at the anchor.)

If TE is sizable, it is fed back with a suitable gain to correct the initial guess at the first tension ($TBOAT$) so that, after a new iteration (or several) no extra tension remains to the right of the anchor and a new time step calculation can be initiated. The proper feedback gain is computed after the first iteration by assuming a linear relationship between the tension change at the boat ($DTBOAT$) and the extra tension change ($TEOLD - TE$) as shown on the simulation flow-chart contained in the next section.

Finally, to complete the formulation of the problem, a set of initial conditions must be given for each lumped mass on the line. Since the equations of motion are of the second order, it is necessary to specify both the positions and velocities at $T = 0$.

In order to obtain the position of each station initially (which should be found to lie on a catenary curve), one can assume that the initial velocity components are zero at each node, and obtain the positions from the equations for static equilibrium of the line starting from any approximated solution of the catenary, provided certain precautions are taken with regard to stability (see section IV). This method, although accurate, requires excessive computer time, especially for the case of a long mooring line with numerous segments where the cable oscillates in the water for a very long period of time before settling toward the equilibrium configuration.

B. Modified Equations for the Elastic Cable

The equations governing the motion of the elastic cable falling in a fluid medium are almost equivalent to those derived in part A of the present section with the exception of equation (2.15). The elastic properties of the cable are introduced by replacing this equation by an expression for Hooke's law. That is, it is assumed that linear stretch is proportional to tension is a good model of the elastic behavior of the cable. In the case of a synthetic line, this assumption is not as good as one might expect. The energy loss due to hysteresis is a significant factor, greater than the effect of longitudinal drag near the bottom of the rope for example. Also, the slope of the stress-strain (related to the spring constant) curves varies greatly with the time rate of change of tension so that two different longitudinal moduli of elasticity could be used as a model, one for the quasi-static stretch of the line and another for rapid vibrational motions. Finally the elastic model of a

synthetic line under tension should include the variation of the cable cross-section which should have the further effect of changing appreciably the drag characteristics of the line.

The following equations are derived for the simple linear elastic rope. (A more detailed analysis for nylon cable may be undertaken in the future).

It is first assumed that the initial equilibrium "elastic" conditions are known, that is, all the segments and node positions are available with their respective tensions for the static spring-mass system. (The initial "elastic" conditions are set up by a special simple program, called ANCHASET, which takes the "stiff" coordinates at initial time and corrects all the values by application of Hooke's law.) One step in time is then taken after having computed all the drag forces acting on the line. After each iteration in time, the stretch of each segment is computed by:

$$\bar{S}EG_k = \bar{X}_{k+1} - \bar{X}_k \quad (2.22)$$

$$\bar{D}ELX_k = \bar{S}EG_k - IL_k \bar{U}SEG_k \quad (2.23)$$

Thus, the new tensions, once all the lumped masses have undertaken a certain motion, are obtained by:

$$\bar{T}E_k = SK_k \bar{D}ELX_k \quad (2.24)$$

SK_k being the spring constant of the k^{th} segment. Equation (2.14) can now be completed to include all the forces acting on the mass k .

$$\bar{F}_k = -\bar{T}E_{k-1} + \bar{T}E_k + \bar{D}_k + \bar{W}_k \quad (2.25)$$

where all the hydrodynamic reactions have been computed as in part A.

Finally, Newton's law of motion is written

$$\bar{A}_k = (\bar{F}_k \cdot \bar{U}SEG_k / MT_k) \bar{U}SEG_k + (\bar{F}_k \cdot \bar{U}VNOR_k / MN_k) \bar{U}VNOR_k \quad (2.26)$$

In this manner, it is fairly obvious that no iterative feed-back is necessary as it was in the case of the non-elastic cable: at the anchor, the "imaginary" tension to the right of this last node is simply set to zero. ($\bar{T}E_{\text{LAST}} = \bar{0}$) so that equation (2.26) is still valid with \bar{F}_{LAST} containing all the forces acting on the anchor.

The reader will note that because of the much simpler form of the tension equation (2.24) and the lack of iteration, the overall computational efficiency appears much greater for the elastic case. Unfortunately, this advantage vanishes when one considers the stability constraints of this calculation method which requires very small time steps. (In fact the elastic system adds one more degree of freedom to the computation.)

III. Description of Computational Procedure

A. Simplified Non-Elastic Model

The complete mooring is divided into different sections according to symmetrical properties. For the non-elastic model, four sections are required:

The first section carries floats (the floats are widely separated)

The second section also carries floats (the floats are closely spaced)

The third section of the mooring has no floats

The last section consists of the anchor

In this manner, the computation is simplified by cycling through the same Newton's law equations of motion for all segments with 4 different sets of constants corresponding to the 4 different mooring sections described above. (A subscript "p" is used in the program to index the different sections.)

All the initial conditions are read from data cards or loaded from a tape data file as is shown on the simplified flow-chart found at the end of the present section. The equations governing the motion of the cable, as derived in the last section, are summarized here. The basic equations of motion are repeated for convenience.

$$\bar{F}_k = -\bar{T}E_{k-1} \bar{D}_k + \bar{W}_k \quad (2.14)$$

$$\bar{T}E_k = \left[-\frac{MT_k}{IL_k} \left| \bar{V}_k - \bar{V}_{k-1} \right|^2 + (MT_k \frac{dV_{k-1}}{dT} - \bar{F}_k) \cdot \bar{U}SEGOLD_{k-1} \right] \left[\bar{U}SEG_k / (\bar{U}SEG_k \cdot \bar{U}SEGOLD_{k-1}) \right] \quad (2.15)$$

$$\bar{A}_k = \left[(\bar{F}_k + \bar{T}E_k) \cdot \bar{U}SEG_k / MT_k \right] \bar{U}SEG_k + \left[(\bar{F}_k + \bar{T}E_k) \cdot \bar{U}VNOR_k / MN_k \right] \bar{U}VNOR_k \quad (2.7)$$

Once the acceleration vector is calculated, the numerical integration of the equations of motion is carried out automatically by using the simple statements;

$$d\bar{V}_k/dT = \bar{A}_k \quad (3.1)$$

$$d\bar{X}_k/dT = \bar{V}_k \quad (3.2)$$

from which numerical values for the velocity \bar{V}_k and the position vector \bar{X}_k are directly obtained if one uses the MAC computer language. The approximate solution to this set of differential equations is accomplished by the Runge-Kutta process. The basic process consists of the following steps ⁴:

1. Establish initial conditions for the dependent and independent variables (\bar{X}_k and \bar{V}_k are the dependent variables and T is the independent).
 2. Specify a value for the increment to be applied to the independent variable.
 3. Evaluate the derivatives for a particular value of the independent variable.
 4. Using the values calculated in step 3, update the dependent variables with respect to the current value of the independent variable.
 5. Update the independent variable.
6. Repeat steps 3 through 5 until true values of the dependent variables have been calculated for the initial value of the independent variable plus the requested increment.

It should be further noted that in order to properly sequence through these functions, the differential equation loop is associated with a counter called the DQPHASE counter and a DIFEQ statement placed at the end of the differential equation loop. The DIFEQ statement has the task of updating all requested dependent variables with respect to the independent variable, and also of updating the independent variable by the specified increment. The DQPHASE is initialized to 0. Each time the DIFEQ statement is encountered, DQPHASE is incremented by one, and the corresponding operations are performed. Each time DQPHASE becomes 4, a full cycle of steps has been completed and the counter is reset to 0.

It is important to understand that the values of all the independent variables are valid only after the full differential equation cycle has taken place. This is the reason for placing a DQPHASE test into the program whenever any variable value is to be printed or utilized in further computation.

The computational procedure, as shown on the simplified flow-chart, can be considered to be divided into two phases. The first phase assumes a consistent set of tensions all along the line and perfect knowledge of all positions and velocities. (This is done by propagating TBOAT from the fixed point to the next lumped masses by using the proper precomputed external forces.) The same phase then involves the numerical integration of the equations of motion (3.1) and (3.2) to predict the node positions one step ahead.

The second phase involves the evaluation of a small tension discrepancy existing at the anchor (constraint boundary condition), from which a first-order correction to TBOAT (DTBOAT) can be obtained. This requires a first tentative iteration to calculate the gradient of TBOAT with respect to the small tension discrepancy at the anchor (TE) as indicated by the feed-back iteration equation:

$$TBOAT_M = TBOAT_{M-1} - TE \frac{\delta TBOAT}{\delta TE} \quad (3.3)$$

$$\text{where } \frac{\delta TBOAT}{\delta TE} = \text{SLOPE} \approx \frac{\Delta TBOAT}{\Delta TE} = \frac{DTBOAT}{DTE}$$

Assuming a linear relationship between DTBOAT and the variation of TE, one only expects a total number of 3 iterations in order to obtain a full consistent set of tensions, (two iterations for the computation of the tension error gradient SLOPE and a third to achieve the necessary corrections.)

B. Modifications of Standard Program to Obtain Transient Motion After Anchor Impact.

The mathematical model of the mooring developed for the simulation of the fall motion is a reasonably good approximation of a real test at sea if the only interest is in cable shapes, duration of fall, and quasi-static tensions. It is no longer valid after the anchor has hit the bottom of the sea. Immediately before anchor impact, the whole line is under tension and must be considered a spring-mass system for the analysis of the impact effect. Immediately after anchor impact, a different set of conditions exists, and the problem must be modified.

The first simple approach to the problem consists in considering the entire line to remain non-elastic except for the last segment adjacent to the anchor. This modification is carried out with very little change to the original program.

Equations (2.7), (2.14), and (2.15) are still used but only 3 iteration cycles are performed with index p . No further computation is done at the anchor ($p=4$) which is assumed to remain in fixed position on the bottom of the sea. When reaching the last segment, two different tension computations must be used. The first one is used if the last line segment is slack (the lengths of the segments are easily calculated by the equation $\overline{SEG}_k = \overline{X}_{k+1} - \overline{X}_k$). If the last segment is slack, its pull is then set to the weight of the last segment, that is, approximately 5 pounds. The second is used if the last segment is found to be taut. Hooke's law is used for calculating the tension after computation of the segment stretch and choice of the proper modulus of elasticity.

The reader may refer to the more detailed modified flow-chart which immediately follows for a better understanding of the computation procedures.

It should be noted that in the case of a mooring system including floats near the boat, consideration of the elastic properties of the cable is almost superfluous since the slack in the line occurring after the anchor impact is taken up by the buoyancy force at the upper part of the mooring line.

C. Programming the Elastic Fall

A more comprehensive approach to the problem posed by the anchor impact effect on the tension histories consists in considering the whole line to be elastic. The corresponding mathematical model of the mooring approaches reality and enables the deduction of conclusions as presented in the next section of this report.

As briefly explained in section 3, the elastic computation is initiated by the ANCHOSSET program. ANCHOSSET uses any "rigid" initial conditions (stored in accessible memory by the ANCKDROP program) and readjusts all the node coordinates according to the existing tensions and the modulus of elasticity of the cable (no correction is performed at the anchor if impact has already occurred). Adjustments should be made on the node at the start of this part of the program to account for the elastic properties of the line but they have been omitted. This omission is of no consequence for the initial fall when the elastic model is used throughout the entire problem. However, errors are inherent for the case where the elastic case solution is started using the initial conditions as derived from the non-elastic drop conditions at anchor impact. Although the node velocities remain unchanged, a set of updated tensions is also calculated by ANCHOSSET. This is carried out by using the same iteration (feed-back) scheme presented in the computational procedure of the non-elastic model (section 3-A), the first TBOAT value assumed being the ANCKDROP initial condition value.

The major set of machine instructions to be used thereafter is formed by equations (2.22) - (2.26) which have already been introduced in section 2. These equations are repeated here for reference:

$$\bar{S}E G_k = \bar{X}_{k+1} - \bar{X}_k \quad (2.22)$$

$$\bar{D}E L X_k = \bar{S}E G_k - I L_k \bar{U}S E G_k \quad (2.23)$$

$$\bar{T}E_k = S K_k \bar{D}E L X_k \quad (2.24)$$

$$\bar{F}_k = -\bar{T}E_{k-1} + \bar{T}E_k + \bar{D}_k + \bar{W}_k \quad (2.25)$$

$$\bar{A}_k = (\bar{F}_k \cdot \bar{U}S E G_k / M T_k) \bar{U}S E G_k + (\bar{F}_k \cdot \bar{U}V N O R_k / M N_k) \bar{U}V N O R_k \quad (2.26)$$

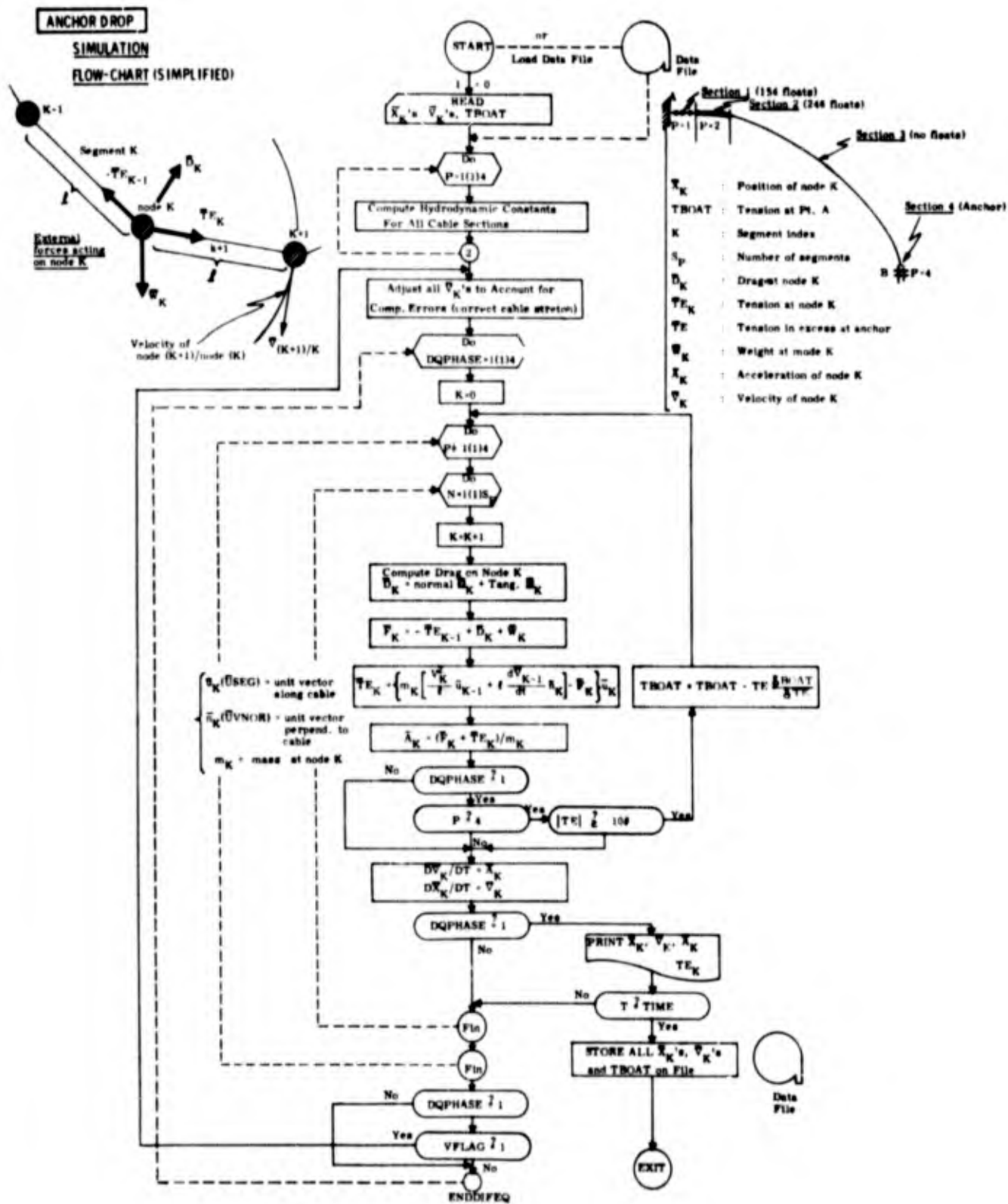


Fig. 4 Simulation Flow Chart (Non-Elastic Case)

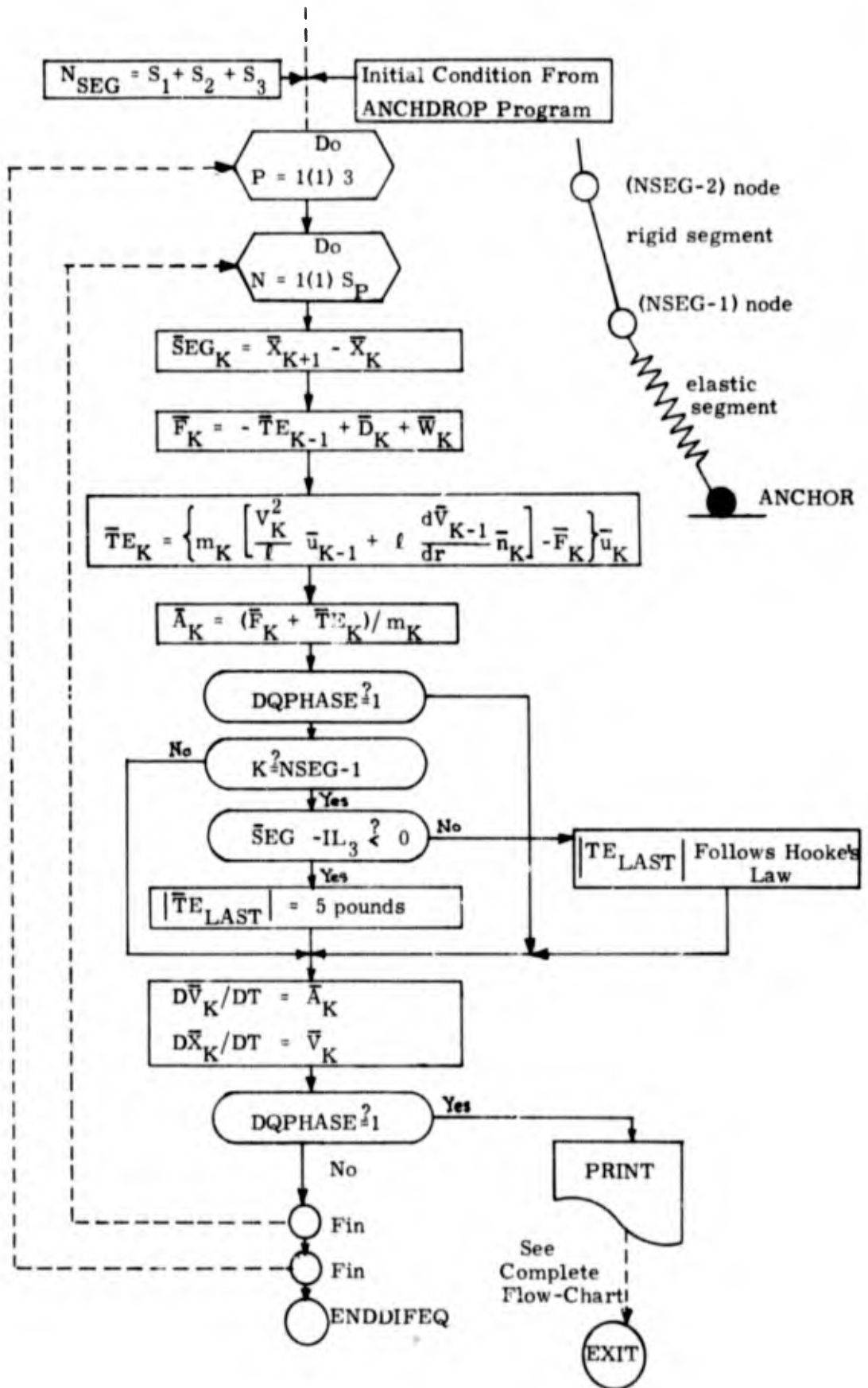


Fig. 5 Simulation Flow Chart (Last Segment Elastic)

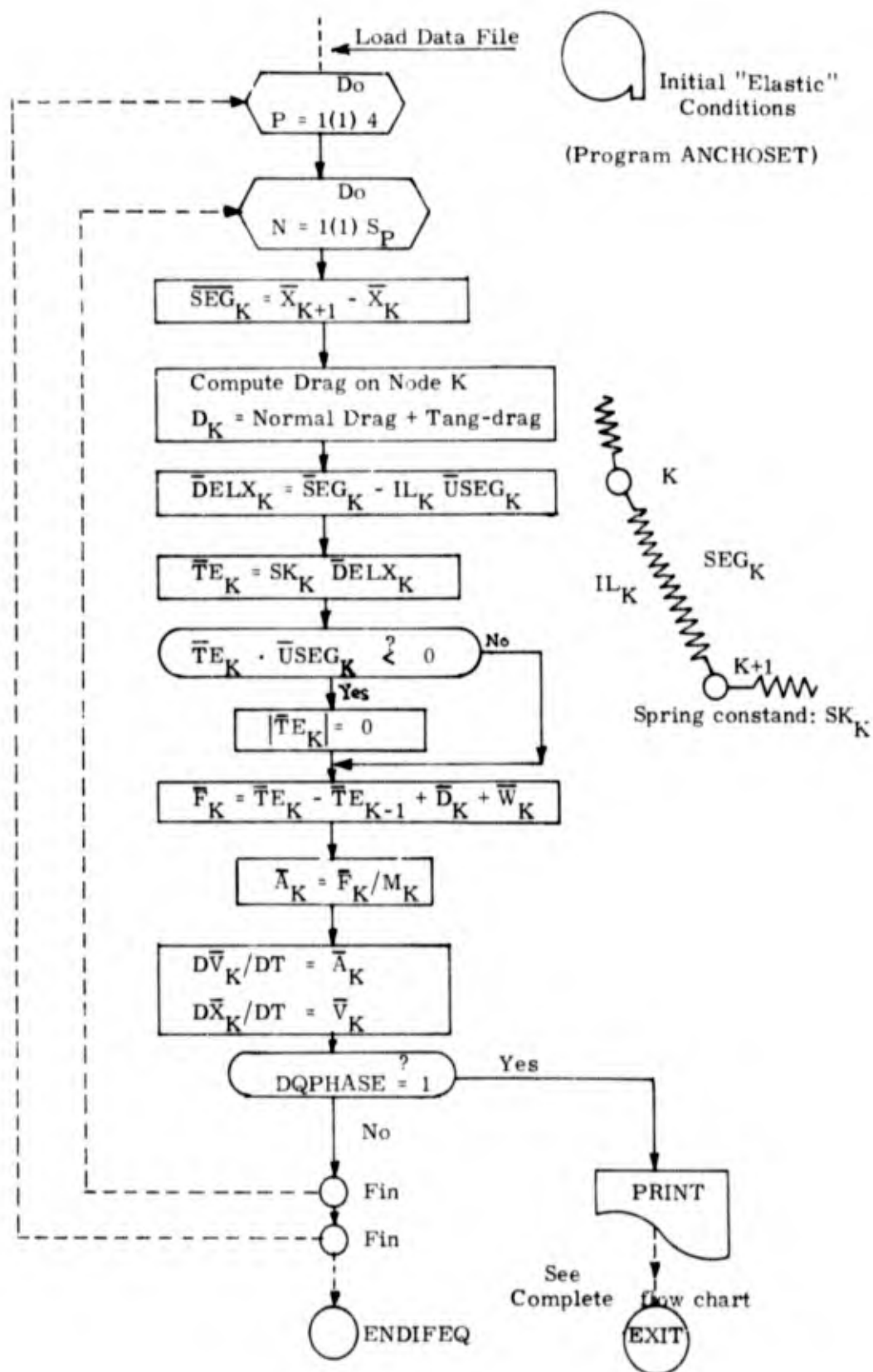


Fig. 6 Simulation Flow Chart (Elastic Case)

As written, equation (2.24) yields positive or negative tensions (using the $\bar{U}SEG_k$ direction as the positive one) depending on the sign of the expression

$$y = \bar{DELX}_k \cdot \bar{U}SEG_k$$

If y is positive, segment k is stretched. If y has a negative value, segment k should be considered slack and thus no tension exists between node k and $(k+1)$. This leads to the nonlinearity shown on the next flow-chart* corresponding to the elastic mooring: $\bar{T}E_k$ is reset to zero whenever segment k is found to be slack. When segment k is stretched, $\bar{T}E_k$ is obtained from the elastic equation (2.24).

It is of interest to note that the use of a dynamic Hooke's law for the elastic properties of nylon cable (taking into account the rate of change of the tension with respect to time) leads to simple modifications in the present program. Equation (2.24) becomes:

$$\bar{T}E_k = SK_k \bar{DELX}_k + DK_k d(\bar{DELX}_k)/dT \quad (3.4)$$

where DK_k is the dynamic spring constant of the nylon cable.

A new differential equation is thereafter necessary, giving the rate of change of \bar{DELX}_k with respect to time.

$$d(\bar{DELX}_k)/dT = (\bar{V}_{k+1} \cdot \bar{U}SEG_k) - (\bar{V}_k \cdot \bar{U}SEG_k) \quad (3.5)$$

The last expression (3.5) thus replaces equation (2.23).

*All the computational flow-charts in this report have been simplified and do not attempt to be self sufficient for the detail of the programs. They have been prepared solely as an aid in understanding the basic calculation process used in the simulations.

IV. Simulation Results

A. Non-Elastic Cable Fall

The original objective of this analysis is the investigation of the deployment of a long mooring at sea. The general characteristics of this long mooring are:

From the boat to the anchor it is composed of:

- A first section of line (1370 feet long) with attached floats (widely separated) steel cable, 117 lbs/1000 ft, (in water) 0.365" diameter cable, 154 spherical floats (buoyancy: 5.25 pounds per float).
- A second section of line (330 feet long) with attached floats (closely spaced) steel cable, 117 lbs/1000 ft (in water), 0.365" diameter, 246 spherical floats (same floats as above).
- A third section of line (4650 feet long) with no floats, steel cable, 117 lbs/1000 ft, (in water) 0.365" diameter.
- An anchor, or coral hook, weighing 2,300 pounds (in water).

The simulation results corresponding to this long mooring will not be presented immediately, but rather will follow those obtained for a shorter line requiring much less computational time and thus enabling a more complete investigation.

Each chart contained within Part A of section 4 is briefly described and may be found after the following explanatory text.

Chart 1: Complete cable shape history of the short mooring simulation. The characteristics of the short line have been chosen to exhibit approximately the same Reynold's numbers as for the original long line during the quasi-static fall. The line is 150 feet long, has a diameter of 0.62 inch and has a spherical anchor which weighs 39 pounds in water.

A normal drag coefficient of 1.8 was used to account for the effect of vortex shedding on the cable. The line was divided into 10 segments and the computation time increments were taken as 0.1 second.

After 60 seconds of fall, it was arbitrarily assumed that anchor impact had occurred, thus the shape of the line was also drawn after a settling period of 20 seconds (60 seconds after initiation). It should be pointed out that the cable shapes obtained near the anchor at the beginning of the fall suffer from the large segment approximation and therefore are not really representative of the real line shape.

Chart 2: Complete tension history at the first node for the 150 foot long line simulation. The tension is also shown after anchor impact and thus requires the consideration of a last elastic segment near the anchor. During the first 8 seconds following the anchor impact, the tension remains approximately constant until the line becomes taut and undergoes elastic oscillations with a period of 0.6 second approximately. The only damping of these oscillations is provided by the tangential drag.

Chart 3: Tension spectra at different times during the fall. The curve 0+ refers to the time immediately after the start of the fall. The tension decrease towards the anchor is primarily due to the weight of the cable. Longitudinal drag has little effect on the tension although it causes some irregularities in the tension steps.

Chart 4: Spectra of velocities along X at different times during the fall for the 150' line.

After 2 seconds of fall, all the cable nodes have very irregular velocities due to the vibrational modes that are excited by large accelerations at the beginning of the fall. However, the vibrations damp out quickly as a consequence of the normal drag forces. This damping provides rapid smoothing to the velocity spectrum curves. Node 5 falls with a velocity which remains almost constant throughout the submerged motion while the anchor velocity decreases rapidly from 10 ft/sec down to 1 ft/sec.

Chart 5: Spectrum of accelerations along X at T=10 sec for the 6500 foot line. This chart refers to some early work undertaken on the large mooring simulation when divided into 75 segments (the number of segments was later reduced to 13 because of computer cost limitation). It shows the vibration modes of the cable. At each node, a sudden acceleration change takes place, giving rise to high frequency oscillations. The frequency of oscillations is thus directly related to the number of segments. Chart 5 clearly indicates that a complete solution of this model would be very expensive.

Chart 6: Complete cable shape history for a 220 foot long line. This chart is quite similar to chart 1 but this time the mooring includes floats at the boat end of the line. The buoyant section of the mooring is divided into 3 segments. The same buoyancy per unit length of cable as for the 7,000' line is used in order to simulate the large mooring behavior. The anchor impact is again assumed to take place after 40 seconds of fall.

Chart 7: Complete tension history at node 1 for the 220 foot long line with floats. This chart is similar to chart 2 but no elastic properties need be considered to obtain the solution after anchor impact. The tension drops immediately after the anchor has hit the bottom, then oscillates with a period approximately equal to 0.3 second. The damping of the tension oscillations is small but considerably higher than in the previous case (last segment is considered elastic).

Chart 8: Tension spectra at different times for the 220 foot long line with floats. This chart may be compared to Chart 3. The presence of the floats creates a tension discontinuity in the vicinity of the third node: To the left of node 3 an added tension exists due to buoyancy forces acting on the line. Note that the highest tensions occur around 10 seconds and not towards the end of the fall as was the result obtained from Chart 2.

Chart 9: History of the velocity along Y at node 12 after anchor impact for the 220' long line with floats.

This chart indirectly shows the transverse oscillations of the cable immediately after the anchor impact and provides suitable criteria to determine the approximate settling time of the cable (around the equilibrium position). It is clear that the line will oscillate for a few minutes before it reaches its rest configuration. The period of oscillation of segment 12 transversely is seen to remain approximately 0.9 second, although the amplitude of oscillation changes appreciably.

Chart 10: Incomplete cable shape history for the long mooring with floats.

Although the computation has not been completed for the entire fall, extrapolations have been made from Chart 6 in order to obtain the expected time of the complete fall (ocean bottom assumed at a 4500 feet depth), as well as the expected settling time of the mooring after anchor impact. Note that during the first two minutes of fall, all nodes from 4 to 9 are found to be above their equilibrium position at time 0. This is due to the large horizontal tension component in the line after anchor drop which overcomes the effect of the cable weight combined with the small vertical tension component (neglecting the affect of drag).

Chart 11: Incomplete tension history at first node for the 6500 foot long mooring with floats.

Again, the tension is only computed during the first four minutes of fall. Extrapolation from Chart 7 permits estimation of the maximum

tension at time = 4.5 minutes, and then the maximum value occurs at node 3 as apparent from Chart 8. On both charts 7 and 11, scant credence should be given to the results obtained in the vicinity of the time origin (as already mentioned for Chart 1), because of the poor correlation of the mathematical model with the physical line immediately after anchor drop.

B. Elastic Cable Fall

The following curves are all related to the short mooring without floats. Most of the elastic analysis is done with a synthetic line. Only the last chart shows the results obtained with a steel cable. In the case of nylon, time steps of the order of magnitude of 0.01 second are used. The time increments have to be at least 100 times smaller for steel cable.

The description of all the "elastic" results will, here again, precede the set of charts placed at the end of this part of section 4.

Chart 12: Tension spectra during the first second of fall of the 150' long nylon line.

At time $0+$, which is the time at which the anchor hits the bottom of the ocean, the tension spectrum is quite regular all along the line. Immediately after impact, elastic tension waves start to propagate back and forth along the line. Segment 2 is seen to remain under relatively high tensions at all times. This may be explained if segment 2 is situated at an anti-node of a stationary wave system. In drawing all the tension spectra charts, the tensions have been assumed to remain constant between nodes and to experience variations only at the nodes, following the simplified mathematical model of the multi-segment line.

Chart 13: Length variation of fifth segment for the 150' long nylon line (first second of fall).

This chart is similar to a tension history chart although tensions have been assumed to remain positive or null at all times during the fall. It is clear that the dynamic stretch of segment 5 is irregular. Also, minimal damping exists in the mathematical model (tangential drag) so that large oscillations are permitted to arise in the vicinity of 0.9 sec. Comparison of the location of the Cartesian coordinates of all the nodes on the elastic line with those on the non-elastic mooring discloses that very little difference exists after the first second of fall of the cable (the comparison has to be made on an average basis in the case of the synthetic line). This result is important: elasticity on the average has little effect on the shapes and time of fall of moorings,

whereas it greatly influences the tension histories.

Chart 14: Tension history at node 2 for the 150' long nylon line after anchor impact.

The tension is seen to oscillate between 100 and 400 pounds. A maximum seems to be reached after 0.3 second.

Charts 15 and 16: Tension spectra for the 160' long nylon line after anchor impact.

These 2 charts provide the reason for drawing the tension history at node 2 (Chart 14): node 2 sustains higher tensions at all times. The time interval between two consecutive spectral figures has been reduced to 0.02 second (as compared with 0.1 second for Chart 12) in order to permit a closer study of the elastic wave propagation. The 0.2 second of time during which the tensions are reproduced here is sufficient to follow the entire history of such an elastic wave as the one appearing to the right of node 3 at 0.02 sec. This wave very clearly travels towards the anchor at high speed (about 625 feet/second) so that higher tensions propagate to the right. At time 0.16 sec the wave end has almost entirely disappeared at the anchor. At time 0.18 sec, the elastic wave has totally vanished and a new wave is about to form to the right of node 5, in the direction of the anchor again. Segment 2 is seen to sustain high tensions at all times.

Chart 17: Tension history at the boat after anchor impact in the case of a steel cable (150' long line).

This chart is drawn from the numerical results obtained from program VIBRATO. This program takes the initial conditions of the cable at anchor impact time both in position and velocity and computes the subsequent coordinates and tensions after collapsing the mooring to one dimension, that is, the line is thereafter assumed rectilinear from boat to anchor impact point as a simplification toward the 10-degree-of-freedom spring-mass problem. (All initial conditions are projected along the boat-anchor line). Negative tensions are permitted in this simplified mathematical model although of not great physical significance. The maximum tension (500 pounds approximately) is seen to be reached after 0.0055 second following the anchor impact. In the time allotted to the present work, it has not yet been possible to run the steel elastic case under the regular ANCKDROP program.

V. Conclusions and Recommendations for Further Studies

The system of nonlinear differential equations describing the free-fall motion of moving systems has been presented and a computational procedure has been given for both the inextensible line and the more general elastic cable. The simulation results include tension histories and cable shapes during the mooring fall motion. Computational cost has limited the study of the elastic line to the first second of fall and also the first second following anchor impact. It is seen that for the elastic case, the time increments used in the numerical simulation have to be very small: 0.01 second for the synthetic line and 0.0001 second for the steel cable.

It is felt that a different mathematical model should be used to describe the initiation of the fall and the mid-portion of the mooring drop. Elastic properties, together with shorter segments are essential for a consistent analysis of the first few seconds of the drop. Similarly, elasticity should be considered a major factor after anchor impact on the sea bottom.

A more complete survey would include the study of the mathematical model itself. Various parameters could be changed, such as the number of segments constituting the line, the moduli of elasticity of the cable and the computational time increments. A better model is also needed for the synthetic line if a precise tension analysis is to be undertaken. More computer runs should be performed for the case of the steel mooring if suitable funding were to be available in the near future. (The computational cost for the steel cable analysis is approximately 100 times that of nylon. For the short 10 segment line, the inextensible program requires 3.2 second of computer time for every second in real time whereas the elastic program in the case of nylon, requires 86 seconds for the same second in real time).

Another analysis of interest would use a better hydrodynamic model for the anchor which has been assumed spherical in the present work. Also more information (and experiment) is needed to design a mathematical model for the hydrodynamic reaction forces where arbitrary numbers or rough approximations have been used. Equally of importance, the program itself should be modified to include the possibility of investigating a non-homogeneous line, that is, a line for which both inextensible and elastic segments may be included. A type of mooring consisting of both nylon and steel is of practical interest and any further analysis in this area should be beneficial to mooring designers.

In an attempt to increase the accuracy of the simulation, some effort should be directed toward a direct computational procedure for solving the partial differential equation system. Two Runge-Kutta integration subroutines may have

to be coupled in a single program, that is, one integration loop in the time domain and another for the integration along the line. This procedure would clearly require considerable computational time and should therefore initially be restricted to short mooring motion analysis.

Finally, a mixed computational method, that is, a method using both analog simulation after anchor impact and fast digital calculation during the free fall of the mooring may well represent a more efficient approach to the problem.

References

1. Glauert, H., "The Stability of a Body Towed By a Light Wire", Aeronautical Research Committee, R & M 1312 (1930).
2. Walton, T. and Polacheck, H., "Calculation of Transient Motion of Submerged Cables", DTMB Report 1279 (1960).
3. Dr. Schlichting, H., "Boundary Layer Theory", McGraw Hill, New York, London, 1960.
4. Users Guide to MAC-360, Instrumentation Laboratory, Massachusetts Institute of Technology, Cambridge, September 1967.
5. Dahlen, J.M., "Oceanic Telescope Engineering Program - Report on Pilot Project Design, Testing, and Progress through October 1968", MIT Instrumentation Lab Report #-2320, November 1968.
6. Little, H.F., "A Stress and Stability Analysis of the Pilot Project Oceanic Telescope", MIT Instrumentation Lab Report E-2321, July 1968.

Appendix A

Programming Notations and Symbols

\bar{A}_k	- acceleration vector at node k (components in feet/sec ²)
AMF	- augmented mass of one float in slugs
AMA	- augmented mass of anchor in slugs
A_N	- equivalent normal area of a cable section
AN_k	- acceleration of node k in the normal direction
A_T	- equivalent transverse area of a cable section
AT_k	- acceleration of node k in the tangential direction
CDN	- normal drag coefficient
CDT	- tangential drag coefficient
DEL_k	- velocity discrepancy due to computational error existing between the two consecutive nodes k and (k+1) in feet/sec
$DELX_k$	- stretch in segment k (for elastic case)
DF	- float drag constant
\bar{D}_k	- drag at node k
* DNC_p	- normal drag constant at each node within section p
\bar{DN}_k	- normal drag force at node k computed from segment k (components in pounds)
dT	- time increment in seconds
DTBOAT	- tension error at the boat in pounds
* DTC_p	- tangential drag constant at each node within section p
\bar{DT}_k	- tangential drag force at node k computed from segment k (components in pounds)
\bar{DT}_{k-1}	- tangential drag force at node k computed from segment (k-1) (components in pounds)
\bar{F}_k	- total force at node k except for tension on anchor side
FTE	- tension error existing to the right of the anchor in pounds
G	- acceleration of gravity in feet/sec ²
IL_p	- length of segment between nodes within section p in feet
L_j	- cable length of the j th section in feet
LUB	- initial depth of anchor (T=0) in feet
* MN_p	- augmented normal mass of one segment within section p in slugs
* MT_p	- augmented tangential mass of one segment within section p in slugs
NF_p	- number of floats in section p
RHOSW	- specific mass of the sea-water in slugs

Programming Notations and Symbols (cont.)

\bar{SEG}_k	vector position difference between nodes k and (k+1)
SK_k	spring constant for the k th segment
S_p	number of segments in section p
SLOPE	ratio of the tension error at the anchor to the tension error at the boat
T	time in seconds
TBOAT	tension at the boat in pounds
\bar{TE}_k	cable tension vector to the right of node k (components in pounds)
UMC	mass of 1 foot of cable in slugs
UMCN	augmented normal mass of one foot of cable in slugs
UMCT	augmented tangential mass of one foot of cable in slugs
* UMN_p	unit normal mass of one segment within section p in slugs
* UMT_p	unit tangential mass of one segment within section p in slugs
\bar{USEG}_k	unit vector along segment k
$\bar{USEGOLD}_k$	unit vector along segment (k-1)
\bar{UVNOR}	unit vector perpendicular to the cable at segment k, directed toward the water surface
UWC	weight of 1 foot of cable (in water) in pounds
\bar{V}_k	velocity vector at node k (components in feet/sec)
\bar{VMP}_k	velocity vector at the midpoint of segment k (components in pounds)
VN_k	normal velocity component at segment k in feet/sec
VT_k	tangential velocity component at segment k in feet/sec
* W_p	weight of each lumped mass within section p in pounds
\bar{X}	position vector at node k (components in feet)
\bar{Z}	unit vector perpendicular to the cable plane completing a right-hand triad with USEG and UVNOR

* When segment k is in section p the value specified for that section applies.

Appendix B

Considerations on Numerical Stability (Non-Elastic Simulation)

Although ordinary differentials have been used exclusively in the program, it should be understood that in strict mathematical terms, the generalized fall motion of a cable in a fluid is governed by a system of partial differential equations, in which the two independent variables are the time T and the curvilinear length S along the line. Both space and time discrete interval approximations enable the treatment of the problem by a system of ordinary differential equations which can be shown to approach the corresponding partial differential equations for the motion of the cable as ΔT and ΔS approach zero.

A rigorous stability analysis may be undertaken using the mathematics of the Runge-Kutta numerical integration procedure based on finite-difference approximations. The strict analysis involves the study of the growth of a small disturbance or perturbation. The conditions for stability are satisfied if the amplitude of a small disturbance, introduced at any time T , in any of the dependent variables, does not increase exponentially with successive time steps. The stability investigation is customarily carried out using the calculus of variations.

The full equation of motion is rewritten by regrouping equations (2.7) and (2.14):

$$\bar{D}_k = \frac{1}{2} (\bar{D}N_{k-1} + \bar{D}N_k + \bar{D}T_{k-1} + \bar{D}T_k) \quad (\text{B.1})$$

$$\bar{F}_k = -\bar{T}E_{k-1} + \bar{D}_k + \bar{W}_k \quad (\text{B.2})$$

$$\begin{aligned} \ddot{\bar{X}}_k = & \left[(\bar{T}E_k + \bar{F}_k) \cdot \bar{U}SEG_k / MT_k \right] \bar{U}SEG_k \\ & + (\bar{T}E_k + \bar{F}_k) \cdot \bar{U}VNOR_k / MN_k \quad UVNOR_k \end{aligned} \quad (\text{B.3})$$

The stability condition may be stated as follows:

If $\delta \bar{Q}(S, T)$ and $\delta \bar{Q}(S, T + \Delta T)$ are values of a variation (or perturbation) in any of the dependent variables X , TE , in the system, then the system is said to be stable, provided:

$$\left| \delta \bar{Q}(S, T + \Delta T) / \delta \bar{Q}(S, T) \right| \leq 1$$

The authors are confident that a complete stability analysis in vector notation could have been performed, although the scope of the present study did not permit the effort. The contemplated approach would have included that introduction of the perturbation $\delta \bar{X}$ and $\delta \bar{TE}$ in the dependent variables X and TE .

In the stability investigation, the following first order approximations were used, where for simplicity, terms involving virtual inertia were omitted (only mass M_k was included):

$$\delta \bar{USEG}_k = \bar{UVNOR}_k \delta \Theta_k \quad (B.4)$$

$$\delta \bar{UVNOR}_k = -\bar{USEG}_k \delta \Theta_k \quad (B.5)$$

Where Θ_k is the rotation angle at segment k (Θ is positive in the counter-clockwise direction).

Equation (B.3) is expanded and the first variation is calculated in the following manner:

$$\begin{aligned} & \delta \left\{ (\bar{TE}_k + \bar{F}_k) \cdot \bar{USEG}_k / M_k \quad \bar{USEG}_k \right\} = \\ & 1/M_k \left\{ \left[(\bar{TE}_k + \bar{F}_k) \cdot \bar{USEG}_k + (\bar{TE}_k + \bar{F}_k) \cdot \delta \bar{USEG}_k \right] \bar{USEG}_k \right. \\ & \left. + \left[(\bar{TE}_k + \bar{F}_k) \cdot \bar{USEG}_k \right] \delta \bar{USEG}_k \right\} \quad (B.6) \end{aligned}$$

If the weight remains constant during the small variation:

$$\delta (\bar{TE}_k + \bar{F}_k) = -\delta \bar{TE}_{k-1} + \delta \bar{TE}_k + \delta \bar{D}_k \quad (B.7)$$

Thus, the first variation system of equations is obtained:

$$\begin{aligned} (1) \quad \delta \bar{X}_k &= 1/M_k \left\{ \left[(-\delta \bar{TE}_{k-1} + \delta \bar{TE}_k + \delta \bar{D}_k) \cdot \bar{USEG}_k + (\bar{TE}_k + \bar{F}_k) \cdot \right. \right. \\ & \left. \bar{UVNOR} \delta \Theta_k \right] \bar{USEG}_k \\ & + \left[(\bar{TE}_k + \bar{F}_k) \cdot \bar{USEG}_k \right] \bar{UVNOR}_k \delta \Theta_k \\ & + \left[(-\delta \bar{TE}_{k-1} + \delta \bar{TE}_k + \delta \bar{D}_k) \cdot \bar{UVNOR}_k - (\bar{TE}_k + \bar{F}_k) \cdot \bar{USEG}_k \right. \\ & \left. \delta \Theta_k \right] \bar{UVNOR}_k \end{aligned}$$

$$- \left[(\bar{T}E_k + \bar{F}_k) \cdot \bar{U}VNOR_k \right] \bar{U}SEG_k \delta \Theta_k \quad , \quad (B. 8)$$

together with the relation:

$$(2) \quad \delta \Theta_k = \left[(\bar{X}_{k+1} + \delta \bar{X}_{k+1}) - (\bar{X}_k + \delta \bar{X}_k) \right] \cdot \bar{U}VNOR_k / \left| \bar{X}_{k+1} + \delta \bar{X}_{k+1} - \bar{X}_k - \delta \bar{X}_k \right| \quad (B. 9)$$

In the above system, $\delta \bar{D}_k = 1/2 (\delta \bar{D}_{k-1} + \delta \bar{D}_k)$ and, assuming that the cable drag coefficient CDN_k remains constant,

$$\delta \bar{D}_k = -2 CDN_k \left| VNOR_k \right| \delta VNOR_k \bar{U}VNOR_k \quad (B. 10)$$

where

$$\delta VNOR_k = (\dot{\bar{X}}_{k+1} - \dot{\bar{X}}_k) \cdot \bar{U}VNOR_k / 2 \quad (B. 11)$$

The following finite difference relations are derived for use in the remainder of this projected analysis:

$$\delta \dot{\bar{X}}_k^{n-1/2} = (\delta \bar{X}_k^n - \delta \bar{X}_k^{n-1}) / \Delta T \quad (B. 12)$$

$$\delta \ddot{\bar{X}}_k^n = (\delta \bar{X}_k^{n+1} - 2 \delta \bar{X}_k^n + \delta \bar{X}_k^{n-1}) / \Delta T^2 \quad (B. 13)$$

Where the superscripts refer to the corresponding computational time steps.

It is further assumed that within a small region in the (S, T) plane, the vectors TE_k^n , F_k^n , etc. vary only slightly, and hence may be treated as constants. Thus, the corresponding indices will now be omitted for clarity in the text ($\bar{T}E^n$, \bar{F}^n etc.).

A solution of the system of equations (B. 8) and (B. 9) can be obtained in the exponential form:

$$\delta \bar{X}_k^n = \bar{a} e^{i\beta k + \alpha n \Delta T} \quad (B. 14)$$

$$\delta \bar{T}E_k^n = \bar{b} e^{i\beta k + \alpha n \Delta T} \quad (B. 15)$$

Where \bar{a} and \bar{b} are real constant vectors, α is complex and β is the angular wave number of the perturbation functions. Substitution into equation (B. 8) will not be performed here because the bracketed expressions become far too lengthy to be reproduced in this report and work on this project was terminated. However, it is

probable that a system of linear homogeneous equations for the vector quantities \bar{a} and \bar{b} could be obtained.

Walton and Poloczek have performed a similar analysis using Cartesian coordinates. They achieved a solution after several algebraic simplifications and manipulations. They finally obtained the characteristic equation of the variational system (similar to equations (B. 8) and (B. 9) but in Cartesian coordinates), namely, as translated into the notation used in this report:

$$M |\bar{S}EG| \lambda^2 + CDN |VNOR| \left[|\bar{S}EG| (1 + \cos \beta) - VT \Delta T (2 i \sin \beta) \right] + 4 TE (\Delta T)^2 \sin^2 (\beta/2) - 2M |\bar{S}EG| \lambda + M |\bar{S}EG| - CDN |VNOR| |\bar{S}EG| \Delta T (1 + \cos \beta) = 0 \quad (B. 16)$$

$$\text{where } \lambda = e^{q \Delta T} \quad (B. 17)$$

The authors have used this characteristic equation to test the validity of their choice of $\Delta T = 0.1$ sec. as follows:

In the case of negligible drag, i. e., $CDN = 0$, approximately, it is seen that equation (B.16) reduces to:

$$\lambda^2 + 4 \left[TE \sin^2 (\beta/2) (\Delta T)^2 / M |\bar{U}SEG| - 2 \right] \lambda + 1 = 0 \quad (B. 18)$$

In order for the solution to be stable, it may be shown that the inequality

$$TE \sin^2 (\beta/2) (\Delta T)^2 / M |\bar{S}EG| \leq 1 \quad (B. 19)$$

must be fulfilled. This requirement is equivalent to the final condition:

$$\Delta T \leq \sqrt{\frac{M |\bar{S}EG|}{TE}} \quad (B. 20)$$

In the more general case, allowing for finite drag, it is possible to show (2) that the requirements for stability are that ΔT satisfies both of the following conditions:

$$\Delta T \leq \sqrt{\frac{M |\bar{S}EG|}{TE}} \quad (B. 20)$$

$$\Delta T \leq \frac{M}{CDN |VNOR|} \quad (B. 21)$$

These two conditions (B. 20) and (B. 21) are both necessary and sufficient to obtain a stable solution.

It should be pointed out that the stability requirement (B. 20) may be derived from mechanical vibration considerations. It simply represents the natural oscillation period of the string - mass system formed by a lumped mass M mounted at the middle of a string of length $2\sqrt{SEG}$ fixed at both extremities.

For the short mooring example presented in Section 4 numerical substitution in the above yields, for a lumped mass of $5/G$ slugs, a segment length of 15 feet, and a tension of 100 pounds, the stability condition:

$$\Delta T \leq \sqrt{\frac{(5/32.2)15}{100}}$$

$$\Delta T \leq 0.152 \text{ second}$$

The second stability condition, using a drag coefficient of 1.8, $RHOSW = 2.08$ (SLUGS/FT³) and a normal velocity component of 2 FT/sec gives:

$$\Delta T \leq \frac{5/32.2}{0.795 \times 2} \quad \text{or} \quad \Delta T \leq 0.098 \text{ sec.}$$

It is clear that when the elastic properties of the line are taken into consideration, the stability of the solution depends primarily on the propagation time of the longitudinal elastic waves. The stability investigation, in this case, involves the determination of the highest vibrational mode of a spring - mass system with many degrees of freedom. It will not be undertaken in this report. It is however clear that very short computational time increments have to be used for the elastic fall, in particular when considering the steel cable.

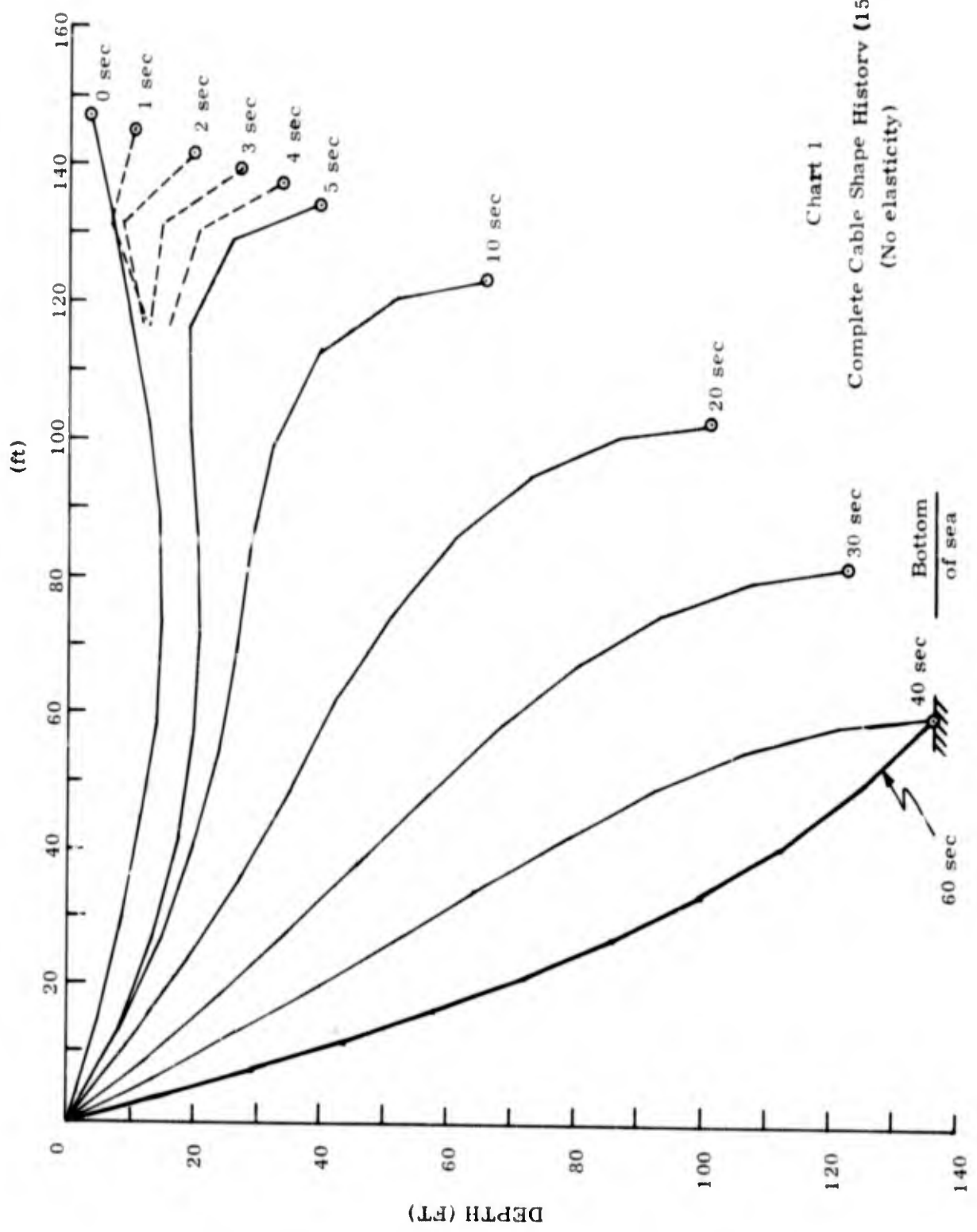


Chart 1
 Complete Cable Shape History (150 ft line)
 (No elasticity)

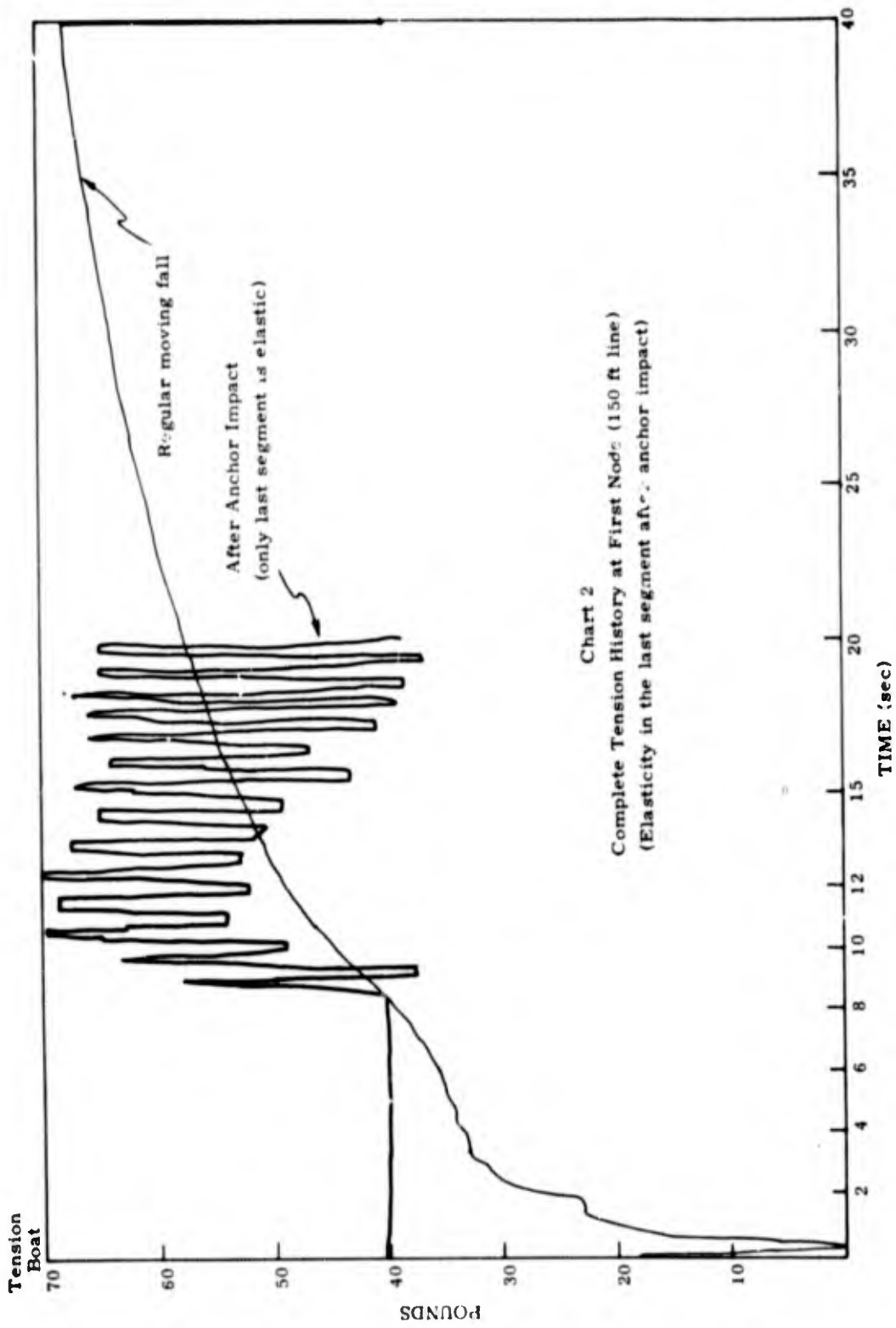


Chart 2
 Complete Tension History at First Node (150 ft line)
 (Elasticity in the last segment after anchor impact)

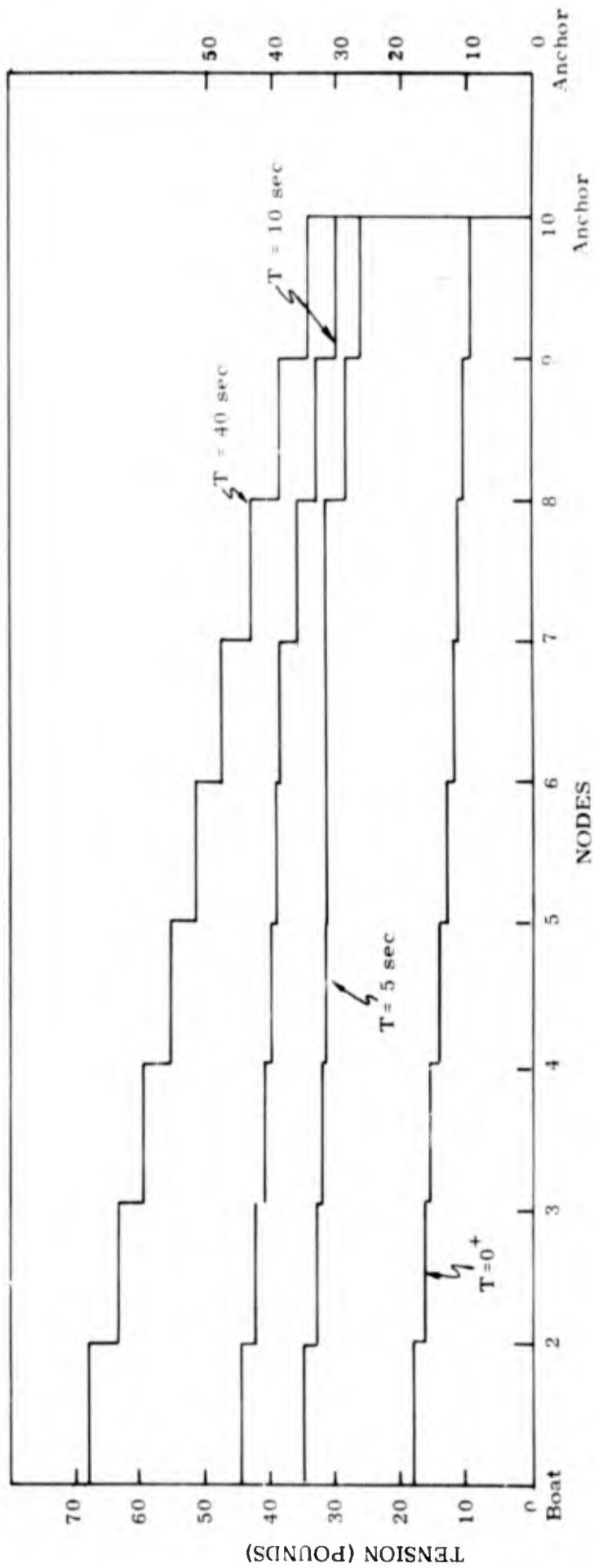
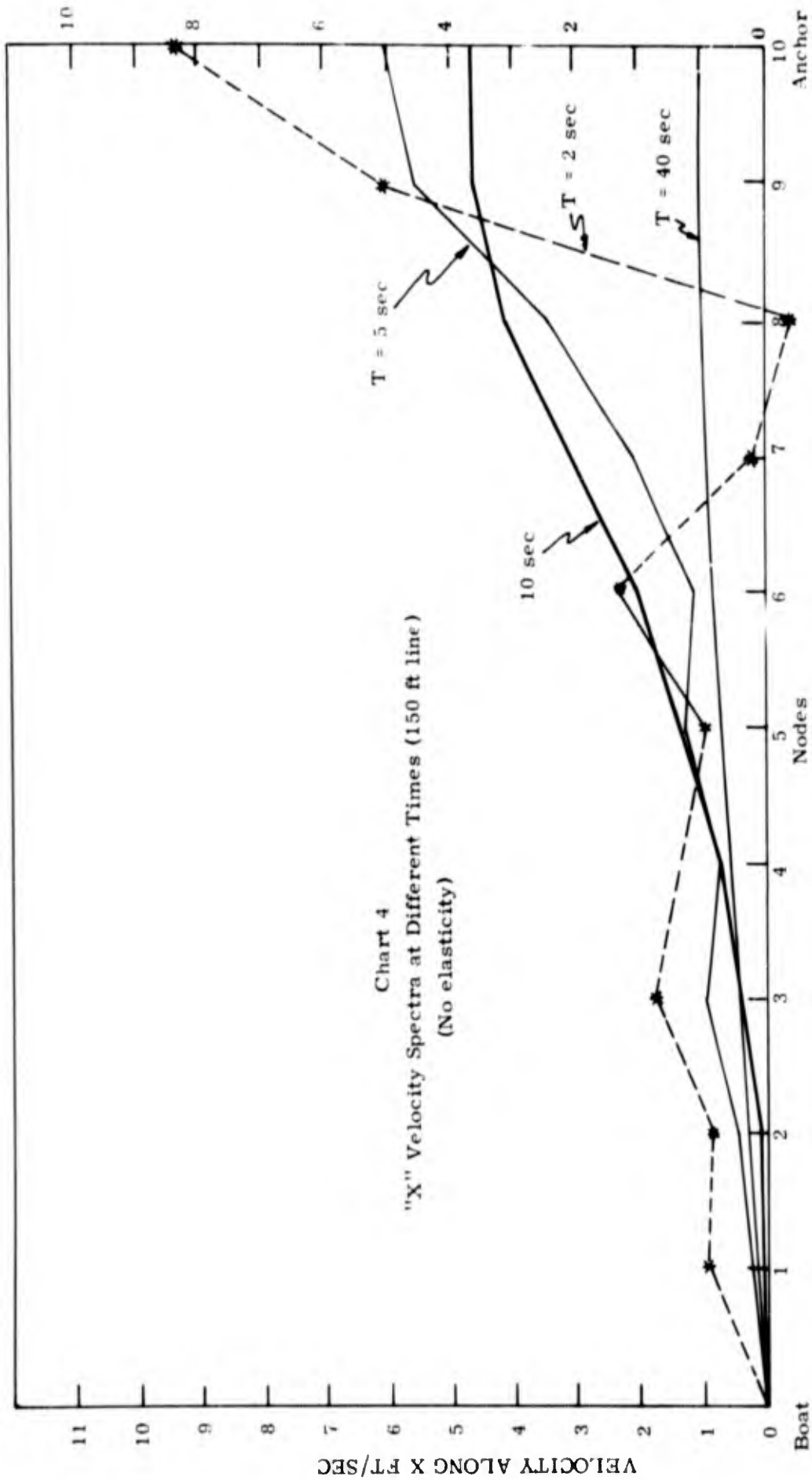


Chart 3
Tension Spectra at Different Times (150 ft line)
(no elasticity)



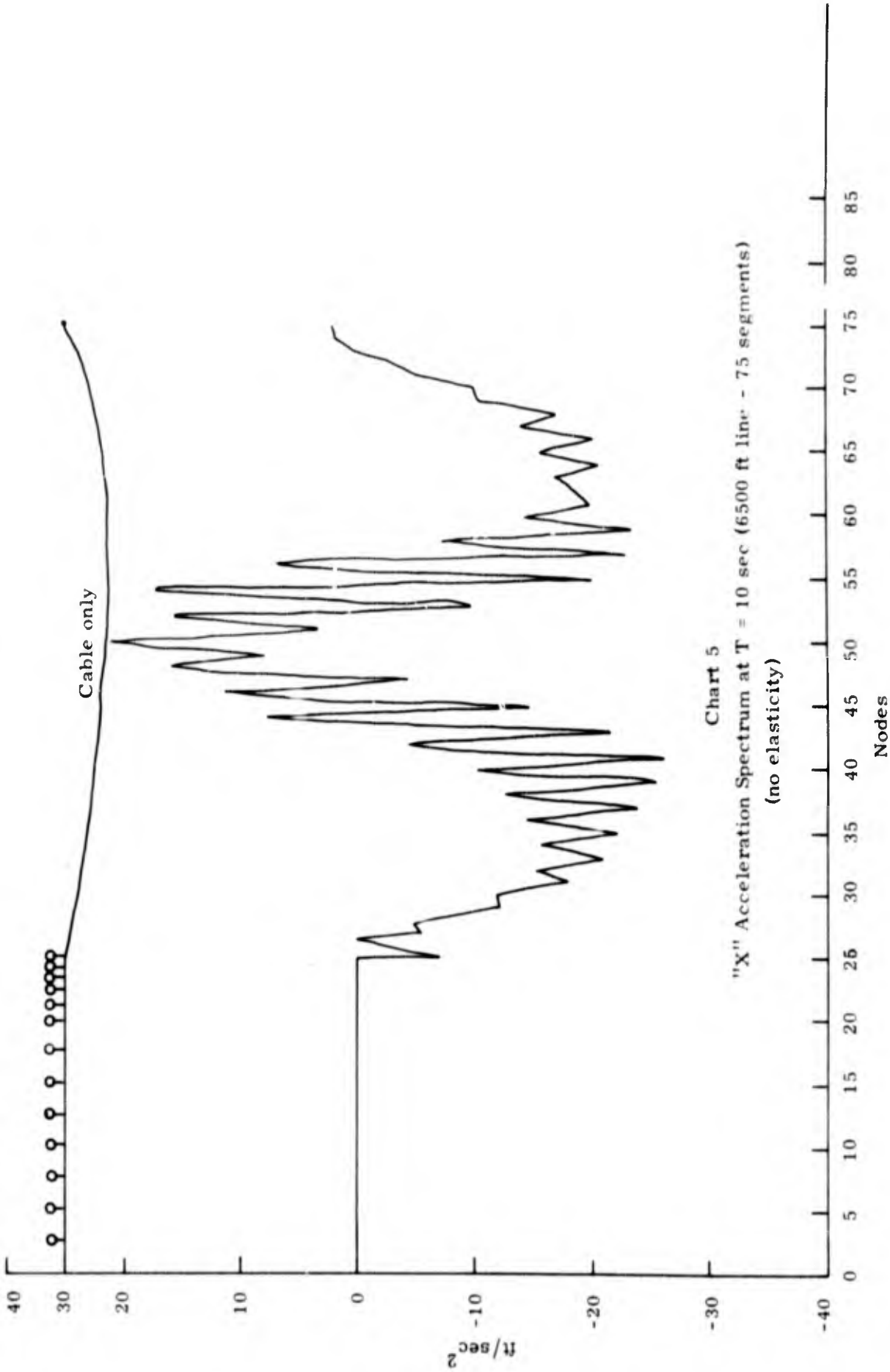


Chart 5
 "X" Acceleration Spectrum at T = 10 sec (6500 ft line - 75 segments)
 (no elasticity)

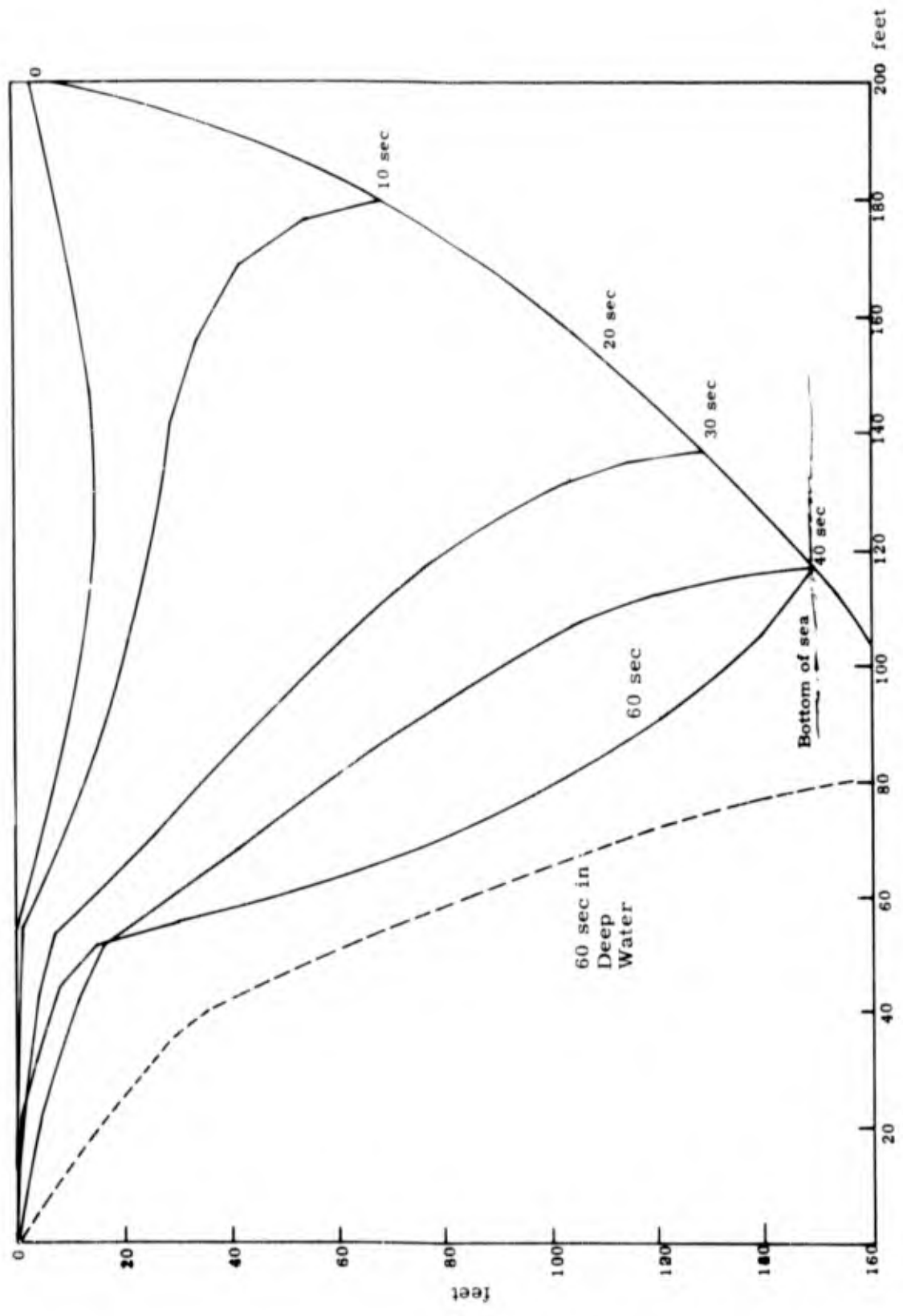


Chart 6
 Complete Cable Shape History (220 ft line) (The line includes floats)

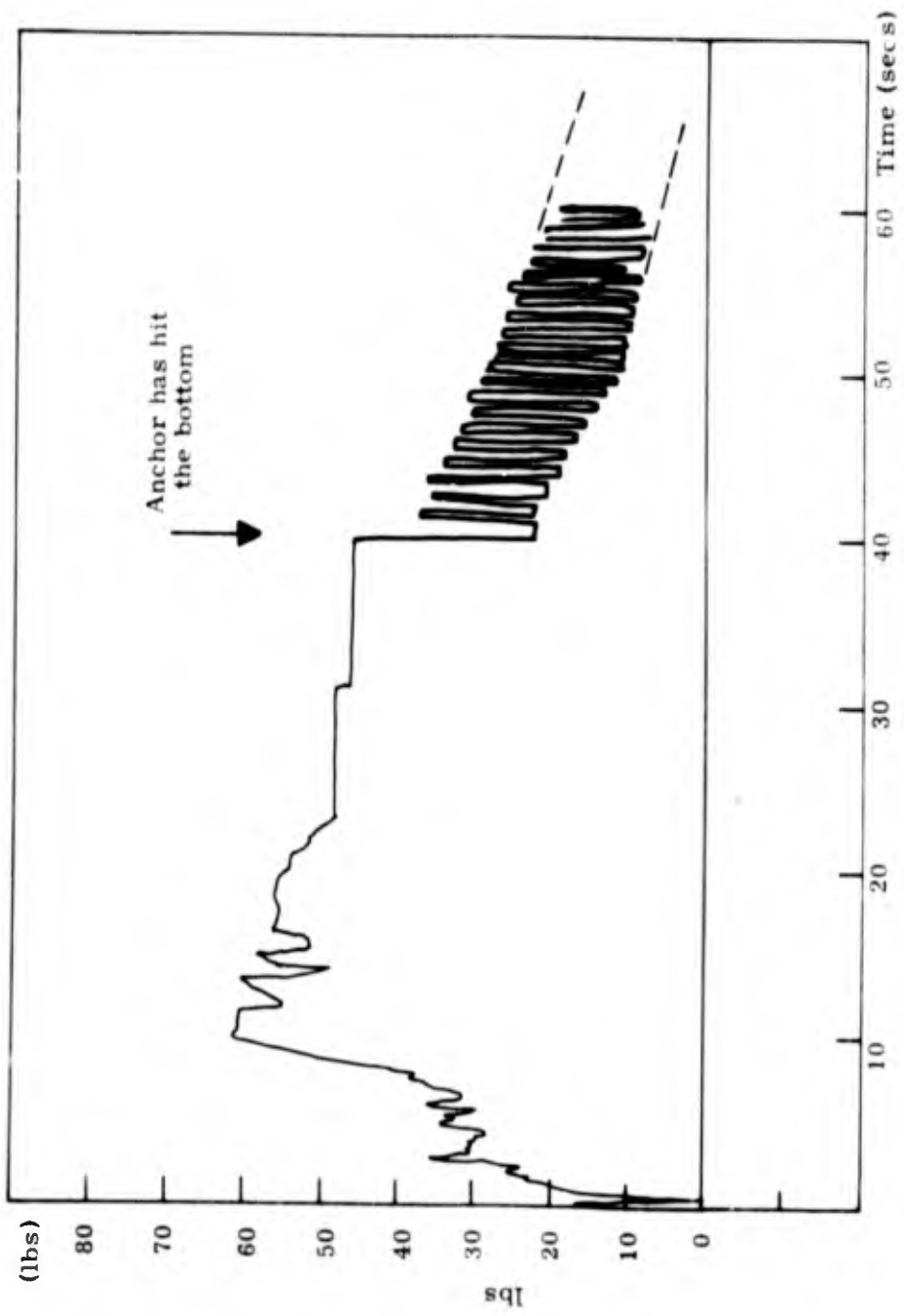
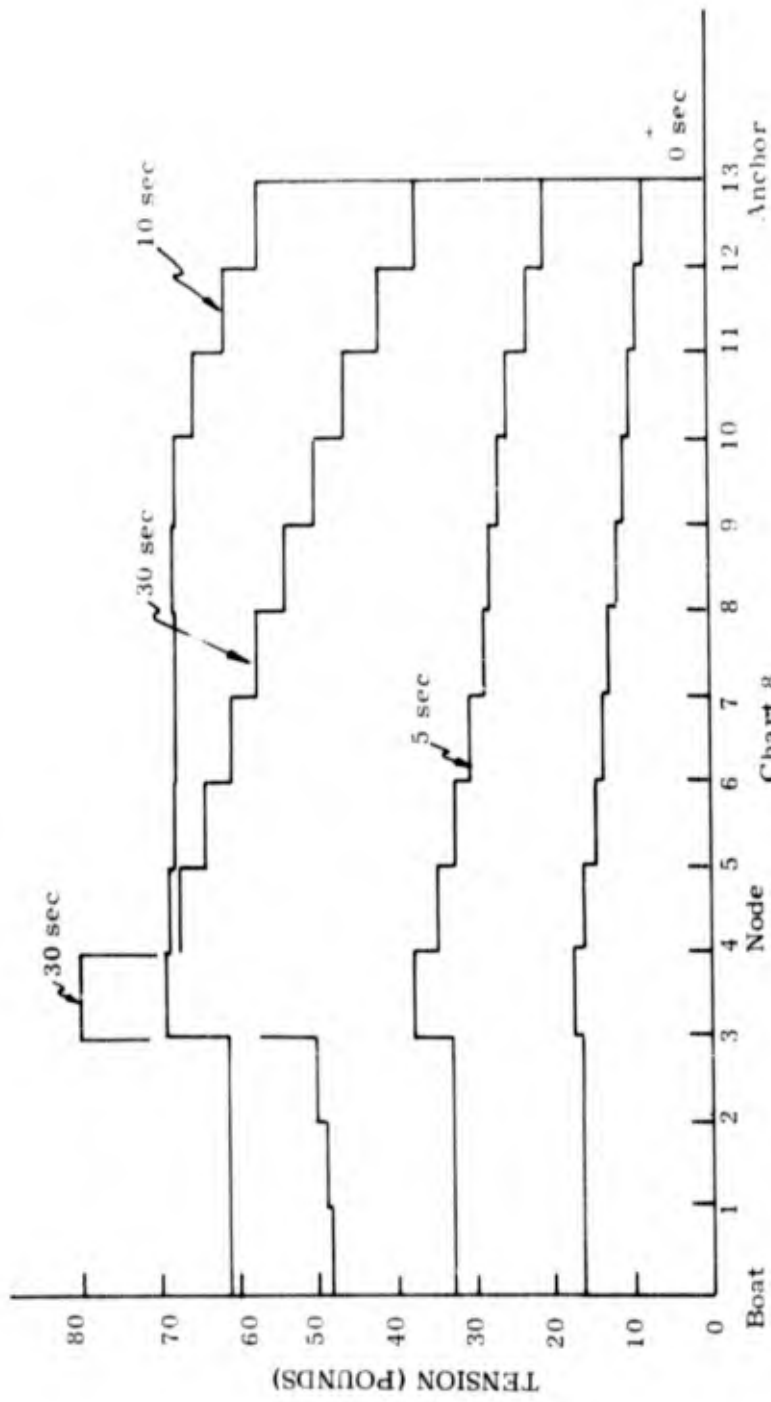


Chart 7
 Complete Tension History at Node 1 (220 ft line with floats)
 (No elasticity necessary)



Tension Spectra at Different Times (220 ft line with floats)
(no elasticity necessary)

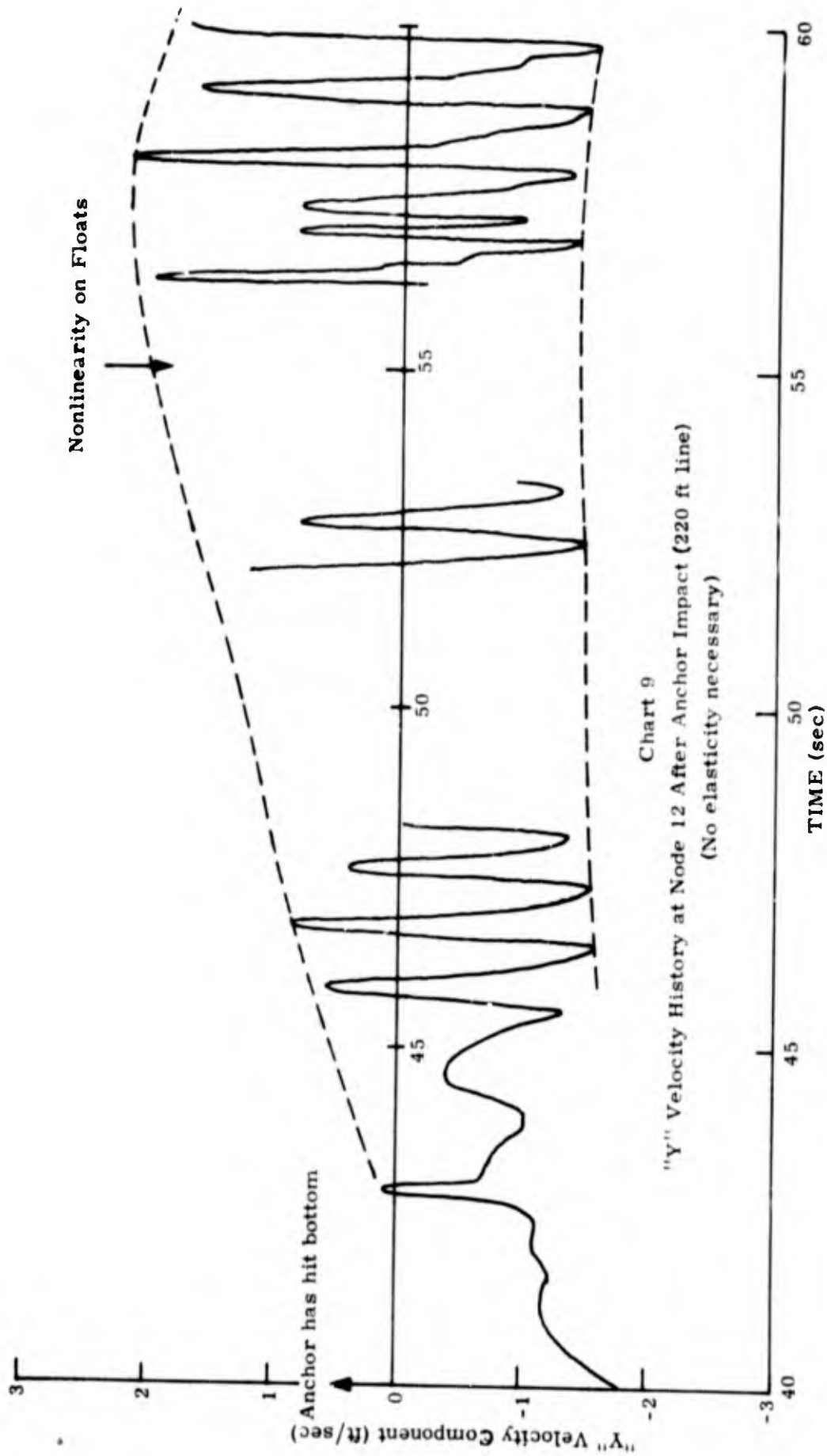


Chart 9
 "Y" Velocity History at Node 12 After Anchor Impact (220 ft line)
 (No elasticity necessary)

Anchor Drop Simulation
(Large Test)

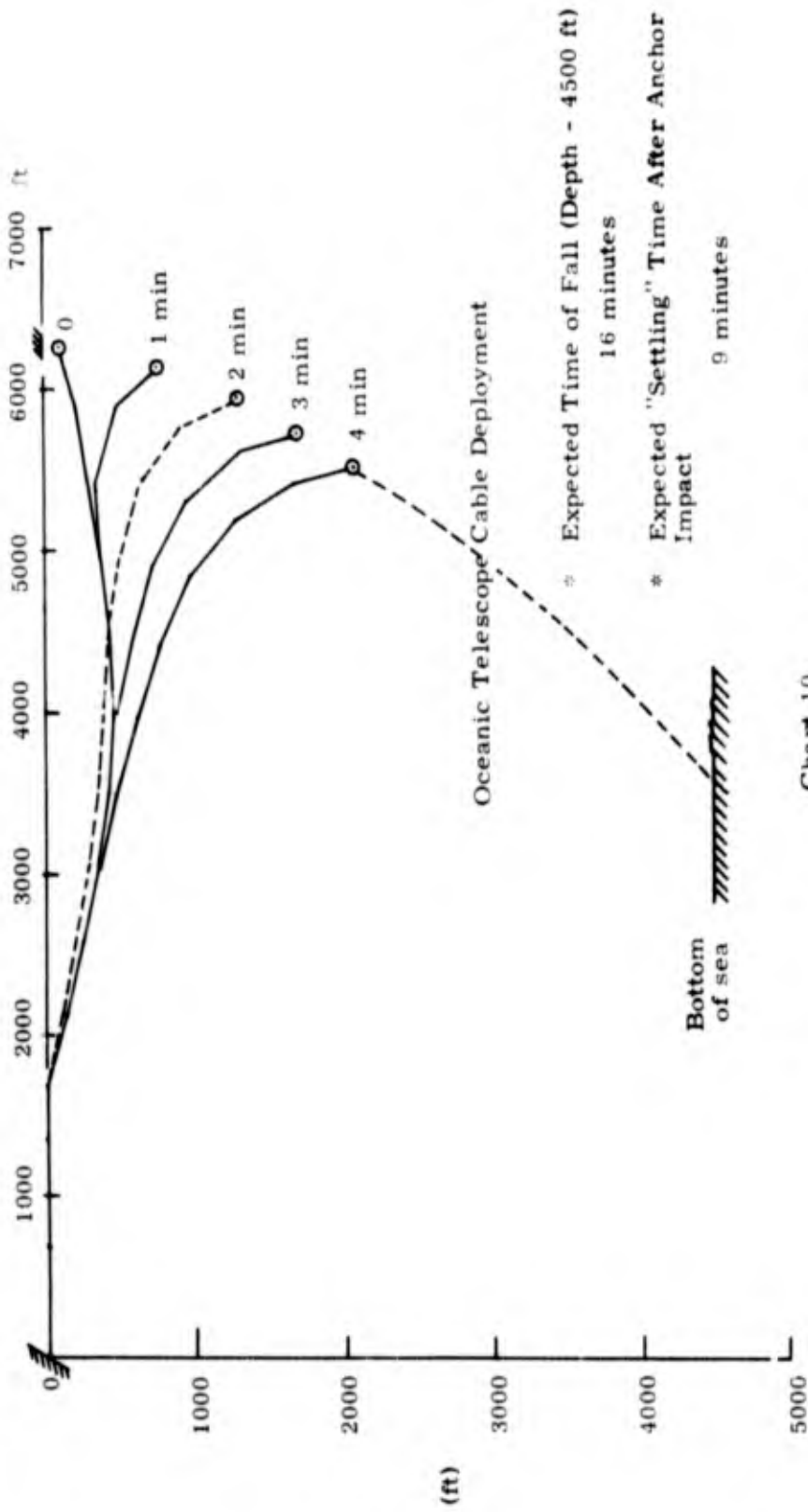
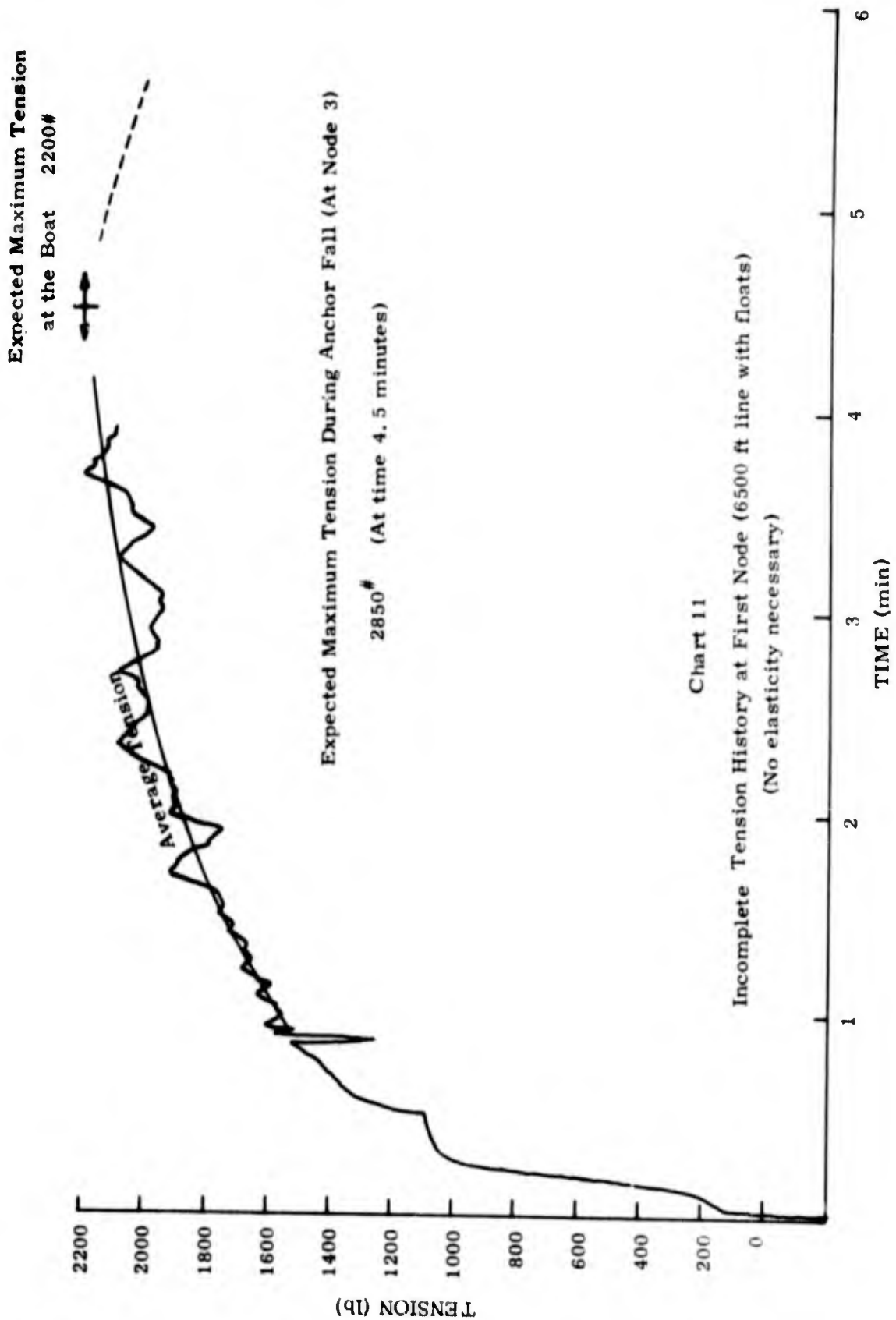


Chart 10

Incomplete Cable Shape History (6500 ft line with floats)
(No elasticity necessary)



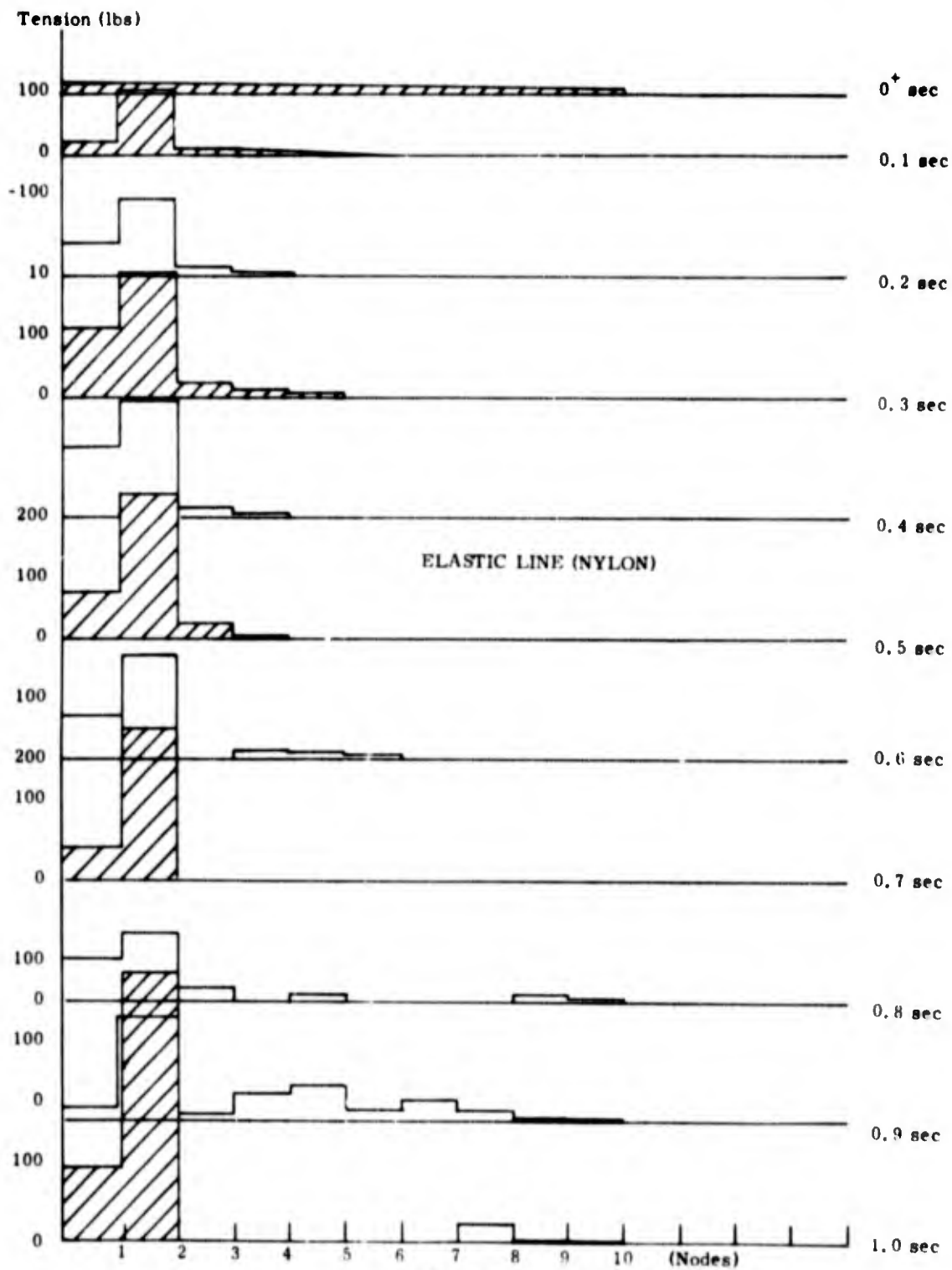
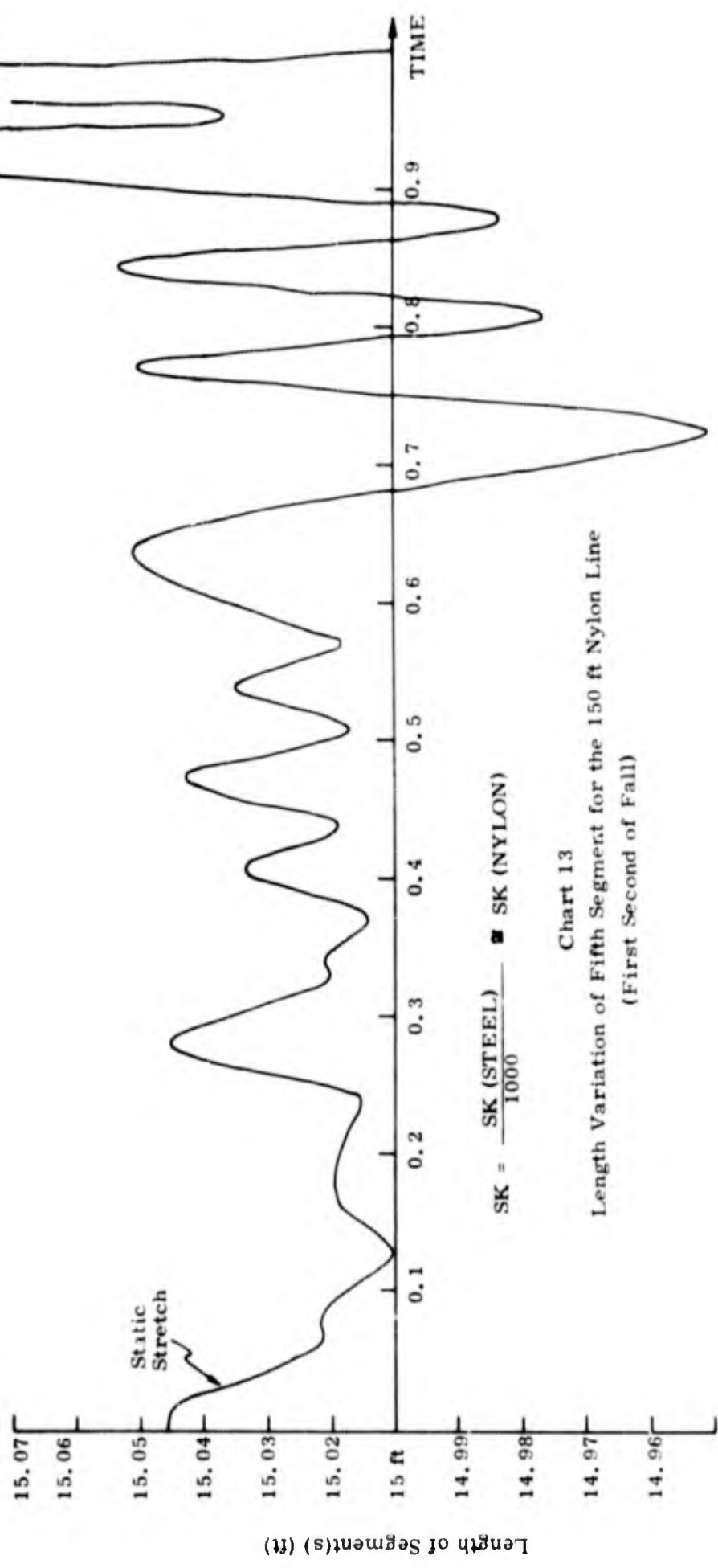
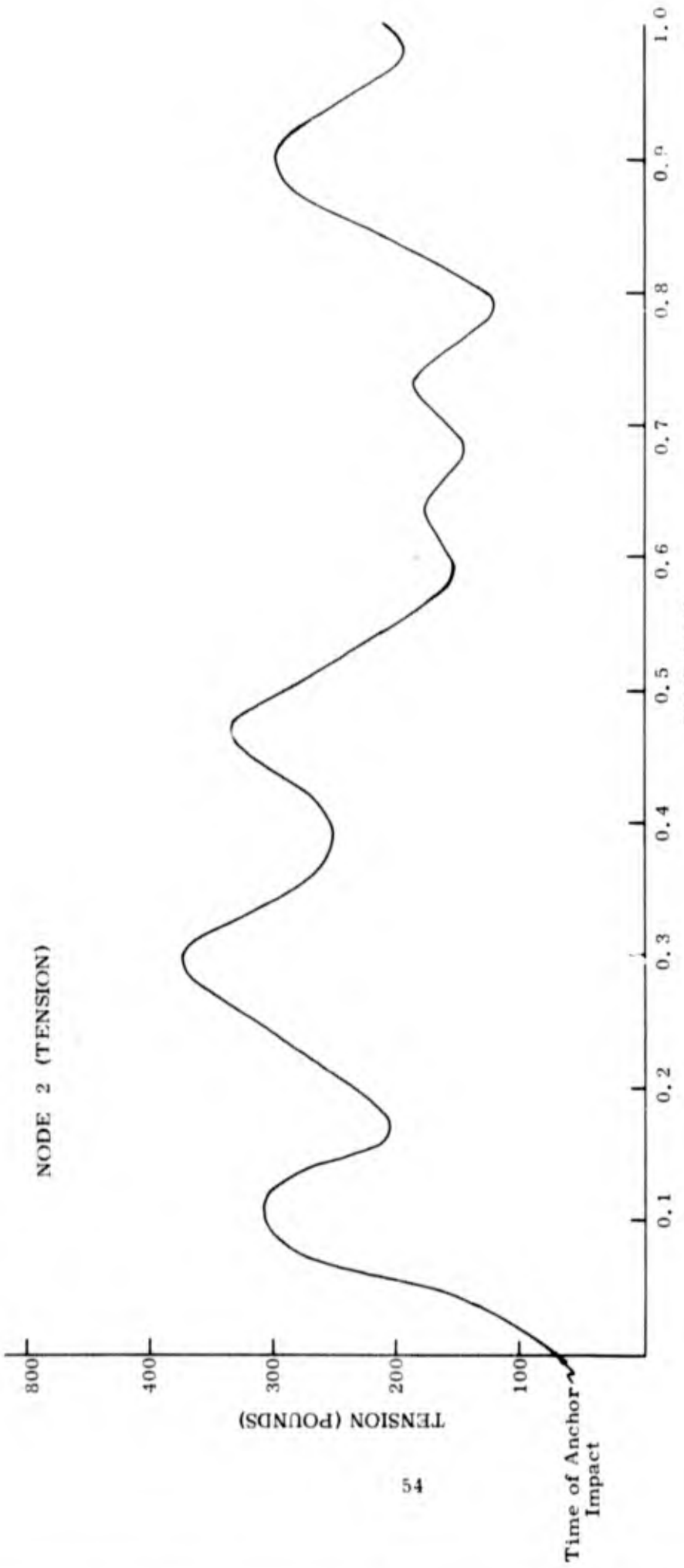


Chart 12
Tension Spectra - First Second of the 150 ft Nylon Line





NODE 2 (TENSION)

TENSION (POUNDS)

TIME (sec)

Chart 14

Tension History at Node 2 for the 150 ft Nylon Line

(After Anchor Impact)

Time of Anchor Impact

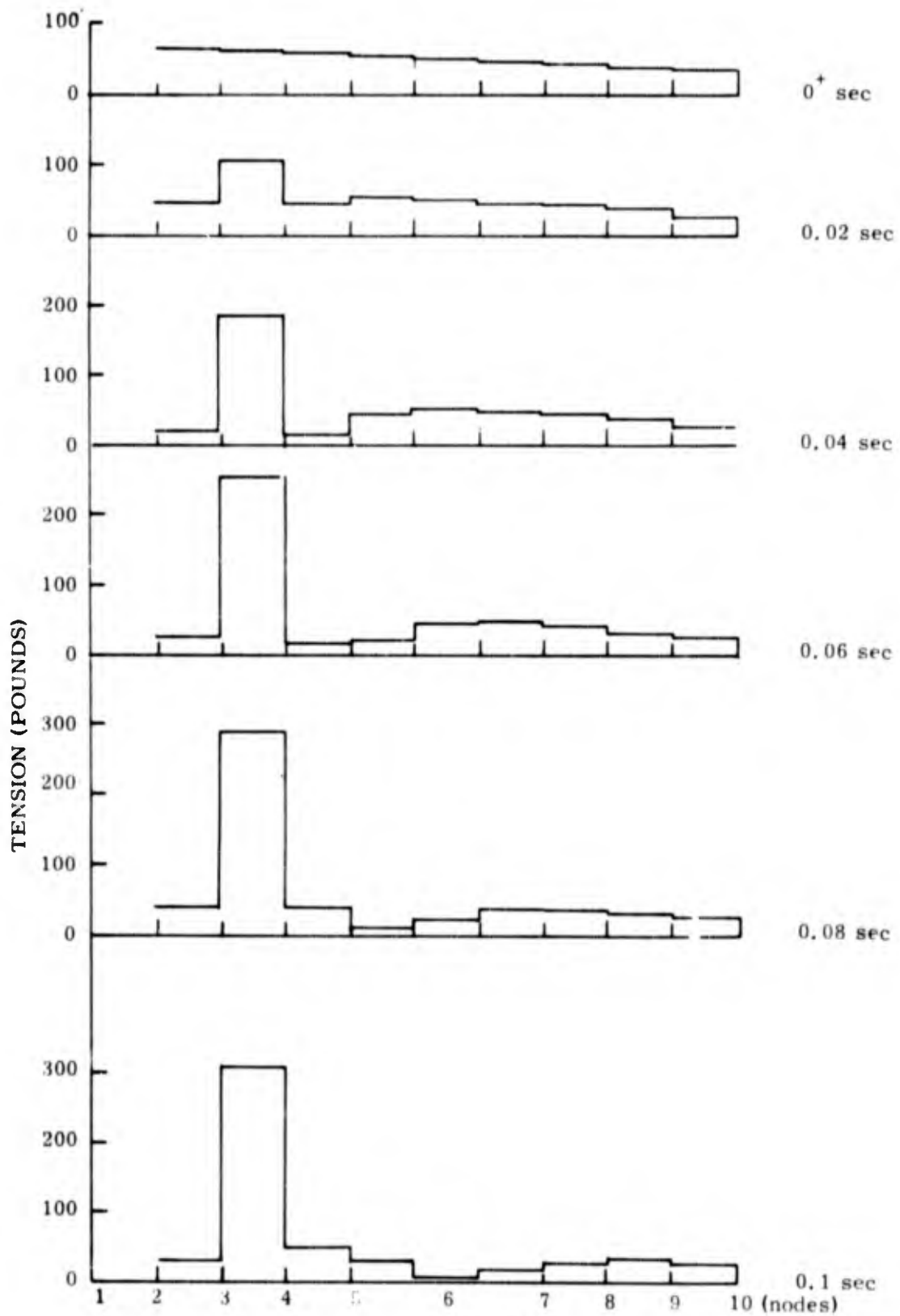


Chart 15

Tension Spectra - 150' Nylon Line After Anchor Impact

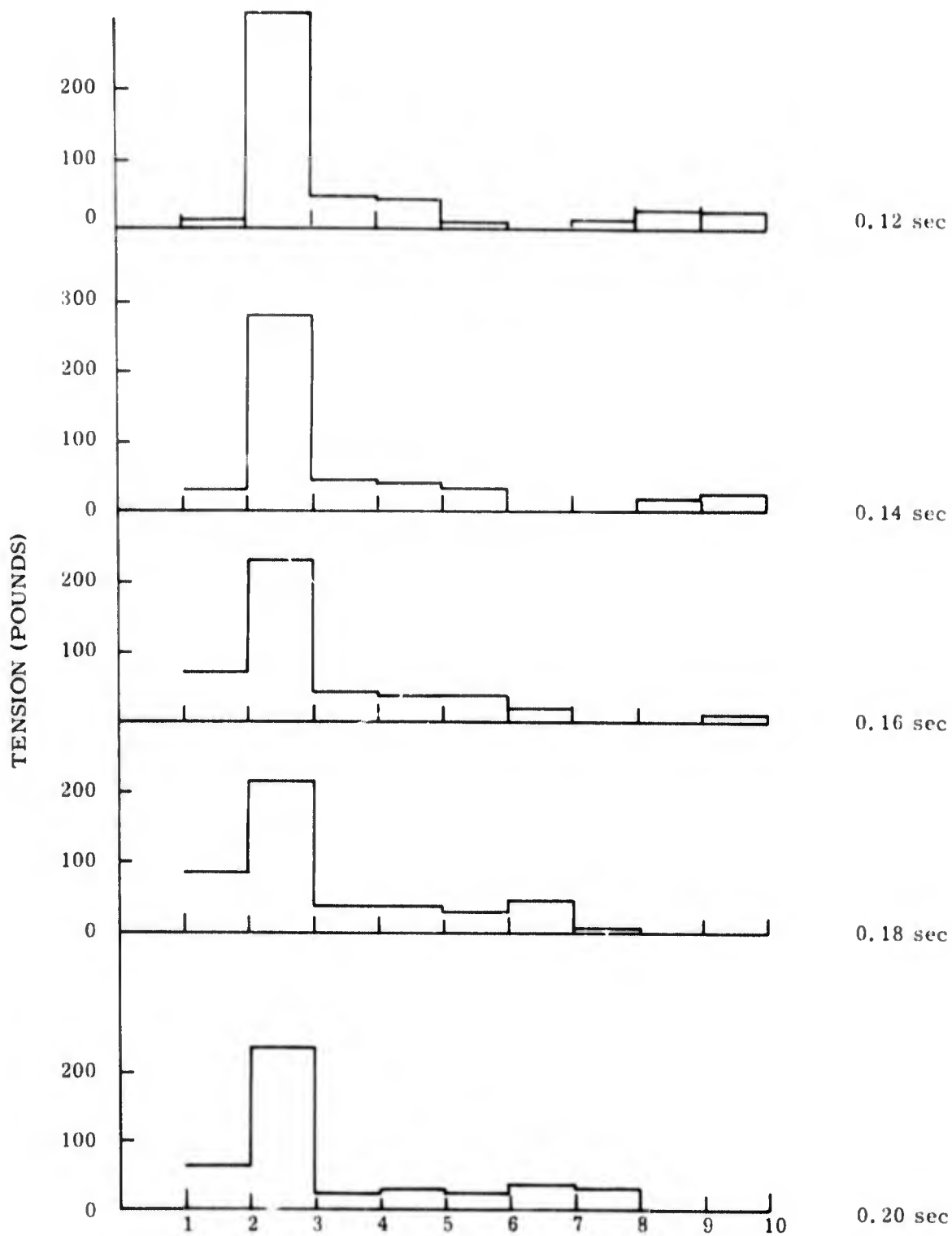


Chart 16
Tension Spectra - 150' Nylon Line After Anchor Impact

STEEL CABLE
Using Vibration Prog.

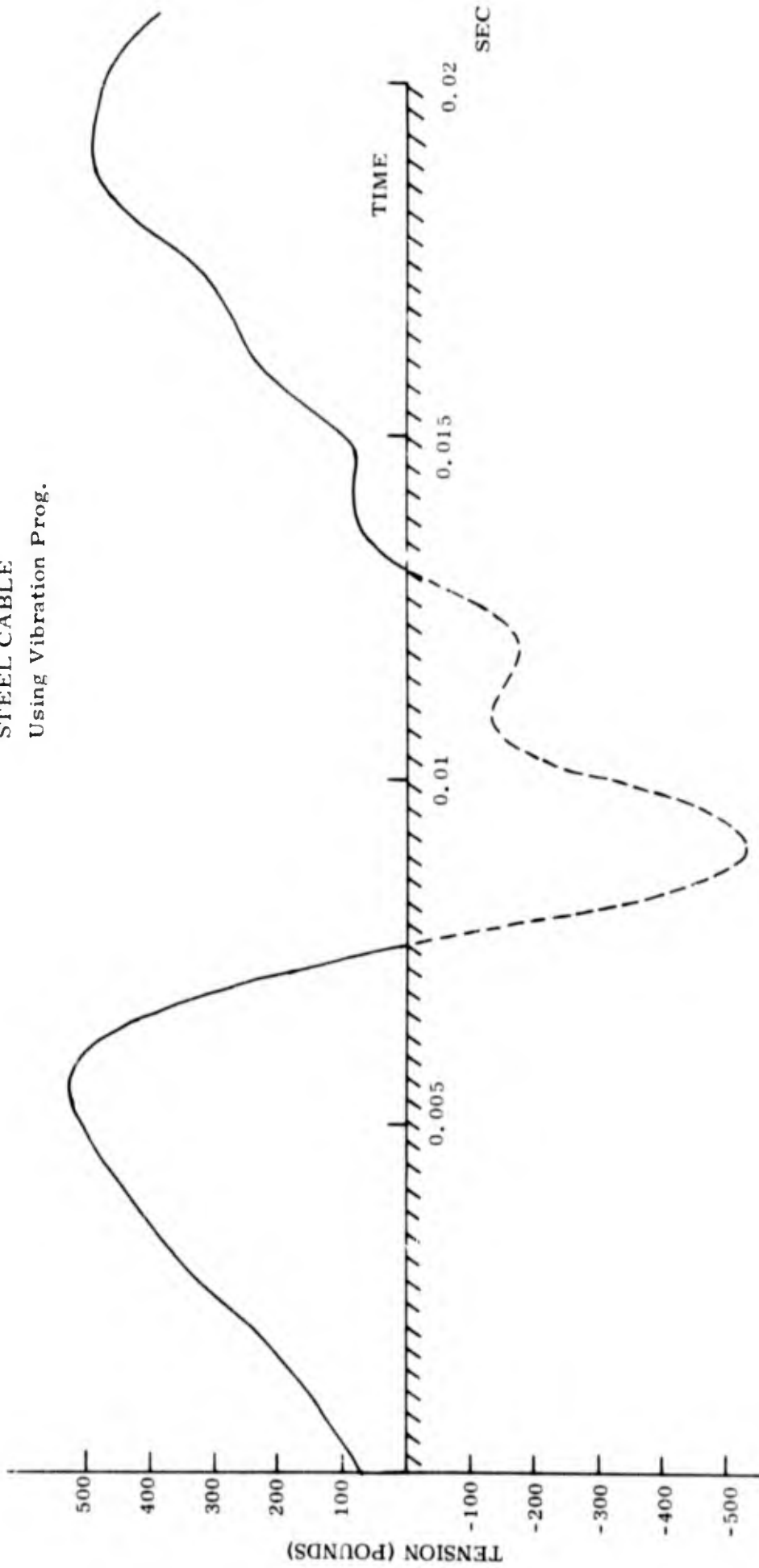


Chart 17
Tension History at the Boat After Anchor Impact (150 ft line)
(Steel Cable)

TIME (secs)